August 3, 2018

New York City, New York

Topobathymetric LiDAR Technical Data Report

Prepared For:

Kristen Grady
The City of New York - NYC DoITT
2 Metro Tech, 4th Floor
Brooklyn, NY 11201
PH: 212-788-6600

Prepared By:

QSI Corvallis
1100 NE Circle Blvd.
Suite 126
Corvallis, OR 97330
PH: 541-752-1204

TABLE OF CONTENTS

Cover Photo: A view looking northwest over Downtown Manhattan in the New York City LiDAR dataset. The image was created from the LiDAR point cloud.

INTRODUCTION

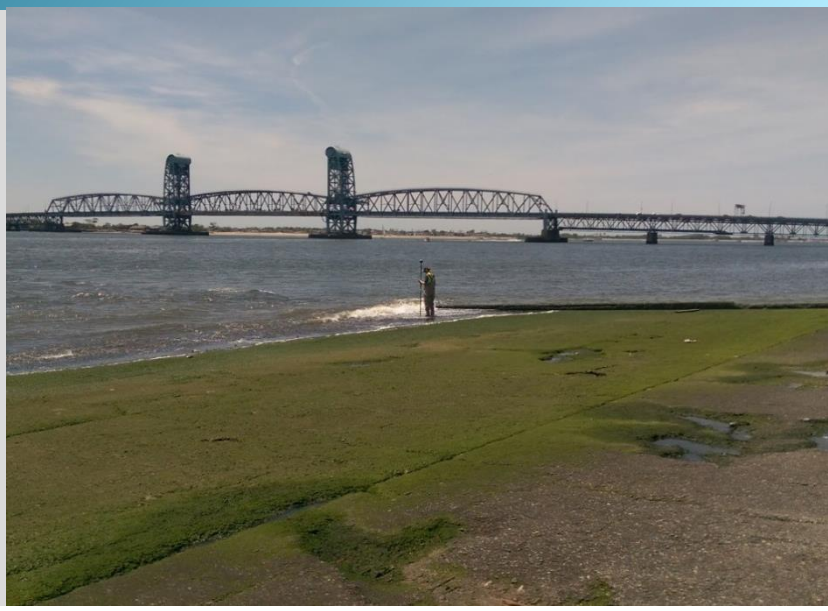

This photo taken by QSI acquisition staff shows a ground professional taking bathymetric check points inside the New York City LiDAR Topobathymetric AOI.

In May 2017, Quantum Spatial (QSI) was contracted by Applied Geographics to collect topographic and topobathymetric Light Detection and Ranging (LiDAR) data for the City of New York (NYC) in the spring and summer of 2017 for the New York City LiDAR project site in New York. QSI collected and processed traditional (near infrared wavelength) LiDAR over the topographic AOI, and spliced together NIR and bathymetric LiDAR (green wavelength) for the topobathymetric AOI. Data were collected to help support the City's many agencies in planning and analysis related to their key initiatives. LiDAR derived DEMs will be crucial for long-term land use planning and assessing the impacts of sea level rise. NYC Parks will be using LiDAR-derived land cover mapping to analyze the need for greening of the city and to help support the measurement of tree canopy height and biomass calculations.

This report accompanies the delivered topobathymetric LiDAR data and documents contract specifications, data acquisition procedures, processing methods, and analysis of the final datasets including LiDAR accuracy and density. Acquisition dates and acreage are shown in Table 1, a complete list of contracted deliverables provided to NYC is shown in Table 2, and the project extent is shown in Figure 1.

Table 1: Acquisition dates, acreage, and data types collected on the New York City Topographic and Topobathymetric LiDAR site

Project Site	Contracted Acres	Buffered Acres	Acquisition Dates	Data Type
Topographic AOI	197,203	208,655	05/03/17, 05/04/17, 05/08/17 - 05/12/17, 05/16/17, 05/17/17	NIR LiDAR
Topobathymetric AOI	56,611	69,554	05/03/17, 05/04/17, 05/09/17 - 05/12/17, 05/16/17, 05/17/17, 07/04/17 - 07/06/17, 07/09/17, 07/10/17, 07/12/17, 07/13/17, 07/22/17, 07/26/17	Spliced NIR and Green LiDAR

Deliverable Products

Table 2: Products delivered to NYC for the New York City Topographic and Topobathymetric LiDAR sites

New York City LiDAR Products Projection: New York State Plane Long Island Horizontal Datum: NAD83 (2011) Vertical Datum: NAVD88 (GEOID012B) Units: US Survey Feet	
Topographic LiDAR	
Points	LAS v 1.4 • All Classified Returns
Rasters	1.0 Foot GeoTiffs (*.tif) • Bare Earth Digital Elevation Models (DEM) • Hydroflattened Bare Earth Digital Elevation Models • Filled Hydroenforced Bare Earth Digital Elevation Models • Unfilled Hydroenforced Bare Earth Digital Elevation Models • Highest Hit Digital Surface Models (DSM) • Intensity Images
Vectors	Shapefiles (*.shp) • Project Boundary • LiDAR Tile Index • DEM Tile Index • Ground Control Shapes • Water's Edge Breaklines • Bridge Breaklines • Hydroenforcement Lines
Topobathymetric LiDAR	
Points	LAS v 1.4 • All Classified Returns
Rasters	1.0 Foot GeoTiffs (*.tif) • Topobathymetric Bare Earth Digital Elevation Models (DEM) • Highest Hit Digital Surface Models (DSM) • Intensity Images

Vectors	Shapefiles (*.shp) • Project Boundary • LiDAR Tile Index • DEM Tile Index • Ground Control Shapes • Water's Edge Breaklines (Hydroflattening, Splicing, Low Tide) • Bridge Breaklines • Bathymetric Coverage Shape
Combined Topographic/Topobathymetric LiDAR	
Points	LAS v 1.4 • All Classified Returns • Unclassified NIR Swaths • Unclassified Green Swaths
Rasters	1.0 Foot GeoTiffs (*.tif) • Combined Topographic/Topobathymetric Bare Earth Digital Elevation Models (DEM) • Combined Filled Hydroenforced Bare Earth Digital Elevation Models • Combined Unfilled Hydroenforced Bare Earth Digital Elevation Models • Combined Highest Hit Digital Surface Models (DSM) • Combined Intensity Images
Vectors	Shapefiles (*.shp) • Project Boundary • LiDAR Tile Index • DEM Tile Index • Ground Control Shapes • Water's Edge Breaklines (Hydroflattening, Splicing, Low Tide) • Bridge Breaklines • Bathymetric Coverage Shape

**The data were created in NAD83 (2011), but for GIS purposes are defined as NAD83 as per New York City specifications.*

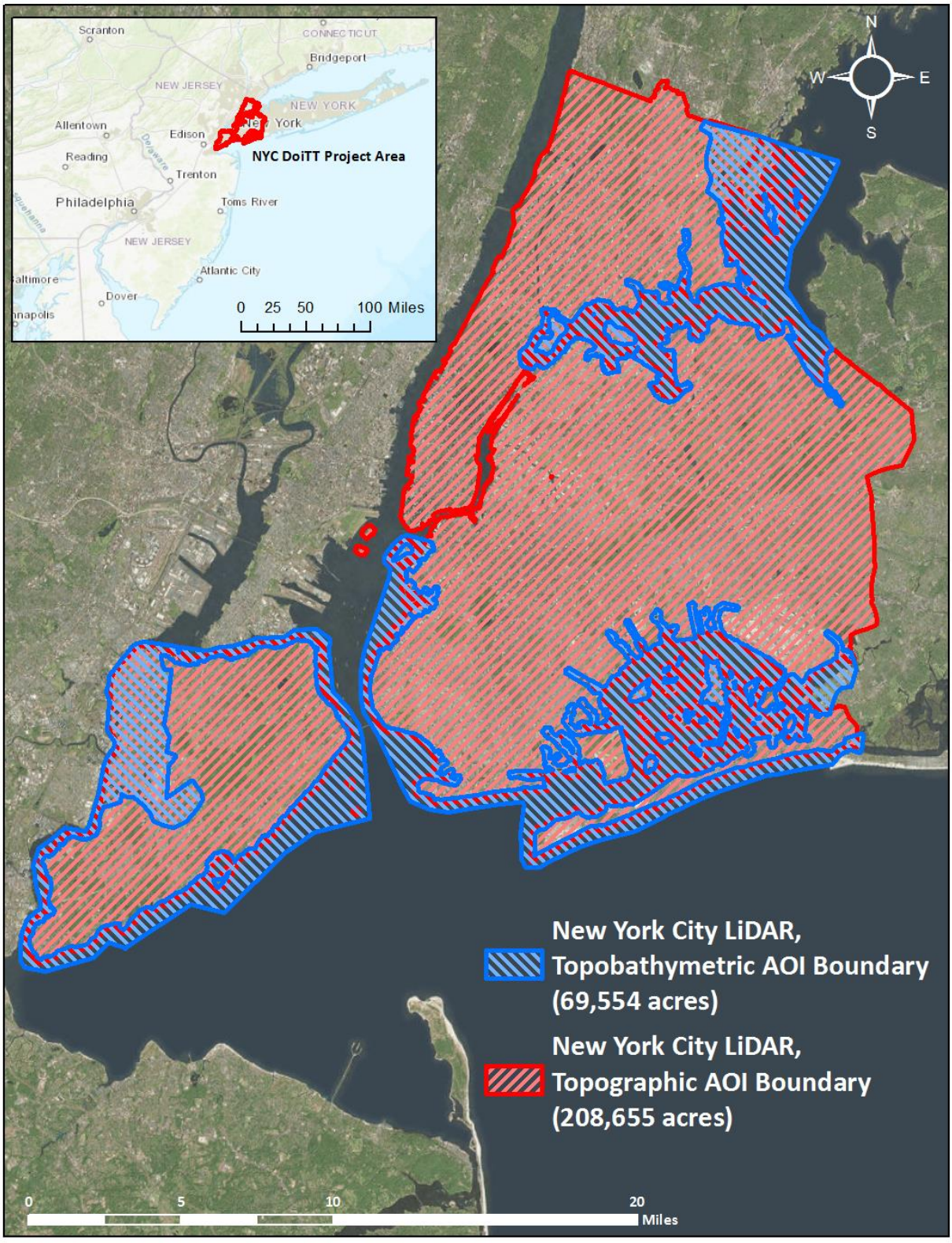

Figure 1: Location map of the New York City Topographic and Topobathymetric LiDAR site in New York

This photo of QSI's pilot inside the Cessna Caravan 208B was taken by QSI's sensor operator during the topobathymetric LiDAR acquisition over New York City.

Planning

In preparation for data collection, QSI reviewed the project area and developed a specialized flight plan to ensure complete coverage of the New York City Topographic and Topobathymetric LiDAR study area at the target point density of ≥8.0 points/m^2. Acquisition parameters including orientation relative to terrain, flight altitude, pulse rate, scan angle, and ground speed were adapted to optimize flight paths and flight times while meeting all contract specifications.

Factors such as satellite constellation availability and weather windows must be considered during the planning stage. Any weather hazards or conditions affecting the flights were continuously monitored due to their potential impact on the daily success of airborne and ground operations. Logistical considerations including private property access, air space restrictions over the City of New York, building heights, and the need to fly at night were carefully managed.

Acquisition was closely coordinated with air traffic control as to not interfere with air traffic from the three major airports in the region. During the topobathymetric flights, tide levels and water clarity conditions were closely monitored to facilitate the best bathymetric bottom return conditions possible. The client requested that all topobathymetric flights were flown at low-tide.

This photo taken by QSI acquisition staff displays the clarity conditions within the New York City Topobathymetric AOI.

Airborne LiDAR Survey

The LiDAR surveys were accomplished using Leica ALS80 and Riegl VQ-880-G laser systems mounted in a Cessna 402C or Cessna Caravan 208B aircraft. The Riegl VQ-880-G uses a green wavelength (ʎ=532 nm) laser that is capable of collecting high resolution vegetation and topography data, as well as penetrating the water surface with minimal spectral absorption by water. The recorded waveform enables range measurements for all discernible targets for a given pulse. Both the Leica ALS80 and Riegl VQ-880-G laser systems can record unlimited range measurements (returns) per pulse. It is not uncommon for some types of surfaces (e.g., dense vegetation or water) to return fewer pulses to the LiDAR sensor than the laser originally emitted. The discrepancy between first return and overall delivered density will vary depending on terrain, land cover, and the prevalence of water bodies. All discernible laser returns were processed for the output dataset. Table 3 summarizes the settings used to yield an average pulse density of ≥8 pulses/m^2 over the New York City Topographic and Topobathymetric LiDAR project areas.

Table 3: LiDAR specifications and survey settings

LiDAR Survey Settings & Specifications			
Survey Area	NIR AOI	Topobathymetric LiDAR AOI	
Acquisition Dates	05/03/2017 – 05/17/2017	05/03/2017 – 07/26/2017	
Aircraft Used	Cessna 402C	Cessna 402C	Cessna Caravan 208B
Sensor	Leica	Leica	Riegl
Laser	ALS80	ALS80	VQ-880-G
Maximum Returns	Unlimited	Unlimited	Unlimited
Resolution/Density	Average 8 pulses/m^2	Average 8 pulses/m^2	Average 15 pulses/m^2
Nominal Pulse Spacing	0.35 m	0.35 m	0.26 m
Survey Altitude (AGL)	1800 m	1800 m	450 m
Survey speed	145 knots	145 knots	120 knots
Field of View	30°	30°	40°
Mirror Scan Rate	48 Hz	48 Hz	80 lines/sec
Target Pulse Rate	314.8 kHz	314.8 kHz	245 kHz
Pulse Length	2.5 ns	2.5 ns	1.5 ns
Laser Pulse Footprint Diameter	39.6 cm	39.6 cm	45 cm
Central Wavelength	1064 nm	1064 nm	532 nm
Pulse Mode	Multiple Pulses in Air (MPiA)	Multiple Pulses in Air (MPiA)	Multiple Times Around (MTA)
Beam Divergence	22 mrad	22 mrad	0.7 mrad
Swath Width	898 m	898 m	327.5 m
Swath Overlap	60%	60%	60%
Intensity	8-bit (Scaled to 16-bit)	8-bit (Scaled to 16-bit)	16-bit
Accuracy	$RMSE_Z \leq 15$ cm	$RMSE_Z \leq 15$ cm	$RMSE_Z \leq 15$ cm

All areas were surveyed with an opposing flight line side-lap of ≥50% (≥100% overlap) in order to reduce laser shadowing and increase surface laser painting. To accurately solve for laser point position (geographic coordinates x, y and z), the positional coordinates of the airborne sensor and the attitude of the aircraft were recorded continuously throughout the LiDAR data collection mission. Position of the aircraft was measured twice per second (2 Hz) by an onboard differential GPS unit, and aircraft attitude was measured 200 times per second (200 Hz) as pitch, roll and yaw (heading) from an onboard inertial measurement unit (IMU). To allow for post-processing correction and calibration, aircraft and sensor position and attitude data are indexed by GPS time.

Manhattan at night, photo taken by a QSI sensor operator during the LiDAR acquisition.

Ground Control

Ground control surveys were conducted to support the airborne acquisition. Ground control data were used to geospatially correct the LiDAR point cloud and used to perform quality assurance checks on final LiDAR data products. In addition, Continuously Operating Reference Stations (CORS) from the New York State Spatial Reference Network (NYSNet) were used to geospatially correct the aircraft positional coordinate data and as base stations for GSP collection. All ground survey work to support the topobathymetric LiDAR acquisition was conducted during the NIR LiDAR collection window.

Base Stations

CORS base stations from the NYSNet were utilized as static base stations for the New York City Topographic and Topobathymetric LiDAR acquisition. The spatial configuration of NYSNet stations and NGS monumentation provided redundant control within 13 nautical miles of the mission areas for LiDAR flights. Base stations and monumentation were also used for the collection of ground survey points using real time kinematic (RTK), post processed kinematic (PPK), and fast static (FS) survey techniques.

CORS and monument locations were selected with consideration for satellite visibility, field crew safety, and optimal location for GSP coverage. QSI utilized ten existing CORS stations and one NGS Monument for the New York City Topographic and Topobathymetric LiDAR project.

Table 4: NYSNet Real Team Network stations used for the New York City Topographic and Topobathymetric LiDAR acquisition. Coordinates are on the NAD83 (2011) datum, epoch 2010.00

CORS ID	Latitude	Longitude	Ellipsoid (meters)
KP14	40° 57' 41.92906"	-74° 07' 52.69137"	7.391
LAMT	41° 00' 16.23300"	-73° 54' 32.05717"	90.181
NYBK	40° 42' 12.32084"	-73° 58' 44.25877"	-15.219
NYBP	40° 42' 03.81683"	-74° 00' 51.54905"	-14.452
NYBR	40° 41' 19.14463"	-74° 00' 04.57867"	-19.038
NYJM	40° 39' 46.05517"	-73° 48' 25.48867"	-12.601
NYOB	40° 33' 05.55502"	-74° 06' 59.66700"	-11.936
NYQN	40° 43' 10.26182"	-73° 43' 48.26660"	-0.403
NYVH	41° 04' 56.22098"	-73° 49' 04.12567"	63.296
ROG_1	40° 38' 21.40078"	-74° 07' 14.42731"	-13.631

Table 5: NGS Monument utilized for the New York City Topographic and Topobathymetric LiDAR acquisition. Coordinates are on the NAD83 (2011) datum, epoch 2010.00

Monument ID	Latitude	Longitude	Ellipsoid (meters)
KU1383	40° 35' 03.58770"	-73° 07' 50.32522"	-29.270

To correct the continuously recorded onboard measurements of the aircraft position, QSI utilized static Global Navigation Satellite System (GNSS) data collected at 1 Hz recording frequency by the base station. During post-processing, the static GPS data were triangulated with nearby Continuously Operating Reference Stations (CORS) using the Online Positioning User Service (OPUS) to verify and update record positions as needed to align with the National Spatial Reference System (NSRS).

Ground Survey Points (GSPs)

Ground survey points were collected using real time kinematic, post-processed kinematic (PPK), and fast-static (FS) survey techniques. For ground survey points collected on May 21, 2017, a Trimble R7 base unit was positioned at a nearby monument to broadcast a kinematic correction to a roving Trimble R8 GNSS or R10 receiver. All other ground survey points were collected using the Real-Time Network to apply kinematic corrections to roving receivers. All GSP measurements were made during periods with a Position Dilution of Precision (PDOP) of ≤ 3.0 with at least six satellites in view of the stationary and roving receivers. When collecting RTK and PPK data, the rover records data while stationary for five seconds, then calculates the pseudorange position using at least three one-second epochs. FS surveys record observations for up to fifteen minutes on each GSP in order to support longer baselines for post-processing. Relative errors for any GSP position must be less than 1.5 cm horizontal and 2.0 cm vertical in order to be accepted. See Table 6 for Trimble unit specifications.

GSPs were collected in areas where good satellite visibility was achieved on paved roads and other hard surfaces such as gravel or packed dirt roads. GSP measurements were not taken on highly reflective surfaces such as center line stripes or lane markings on roads due to the increased noise seen in the laser returns over these surfaces. GSPs were collected within as many flightlines as possible; however the distribution of GSPs depended on ground access constraints and monument locations and may not be equitably distributed throughout the study area (Figure 2).

Table 6: Trimble equipment identification

Receiver Model	Antenna	OPUS Antenna ID	Use
Trimble R7 GNSS	Zephyr GNSS Geodetic Model 2 RoHS	TRM57971.00	Static*
Trimble R8	Integrated Antenna R8 Model 2	TRM_R8_GNSS	Rover
Trimble R10	Integrated Antenna R10	TRMR10	Rover

**Utilized on 5/21/17 only, all other GSPs collected using Real Time Network corrections*

Land Cover Class

In addition to ground survey points, land cover class check points were collected throughout the study area to evaluate vertical accuracy. Vertical accuracy statistics were calculated for all land cover types to assess confidence in the LiDAR derived ground models across land cover classes (Table 7, see LiDAR Accuracy Assessments, page 29).

Table 7: Land Cover Types and Descriptions

Land cover type	Land cover code	Example	Description	Accuracy Assessment Type
Tall Grass	TALL_GRASS		Herbaceous grasslands in advanced stages of growth	VVA
Shrubland	SHRUB		Areas dominated by shrubs	VVA
Forest	FORESTED		Forested areas dominated by deciduous species	VVA
Bare Earth/Urban	BARE, URBAN		Areas of bare earth surface in an urban setting	NVA

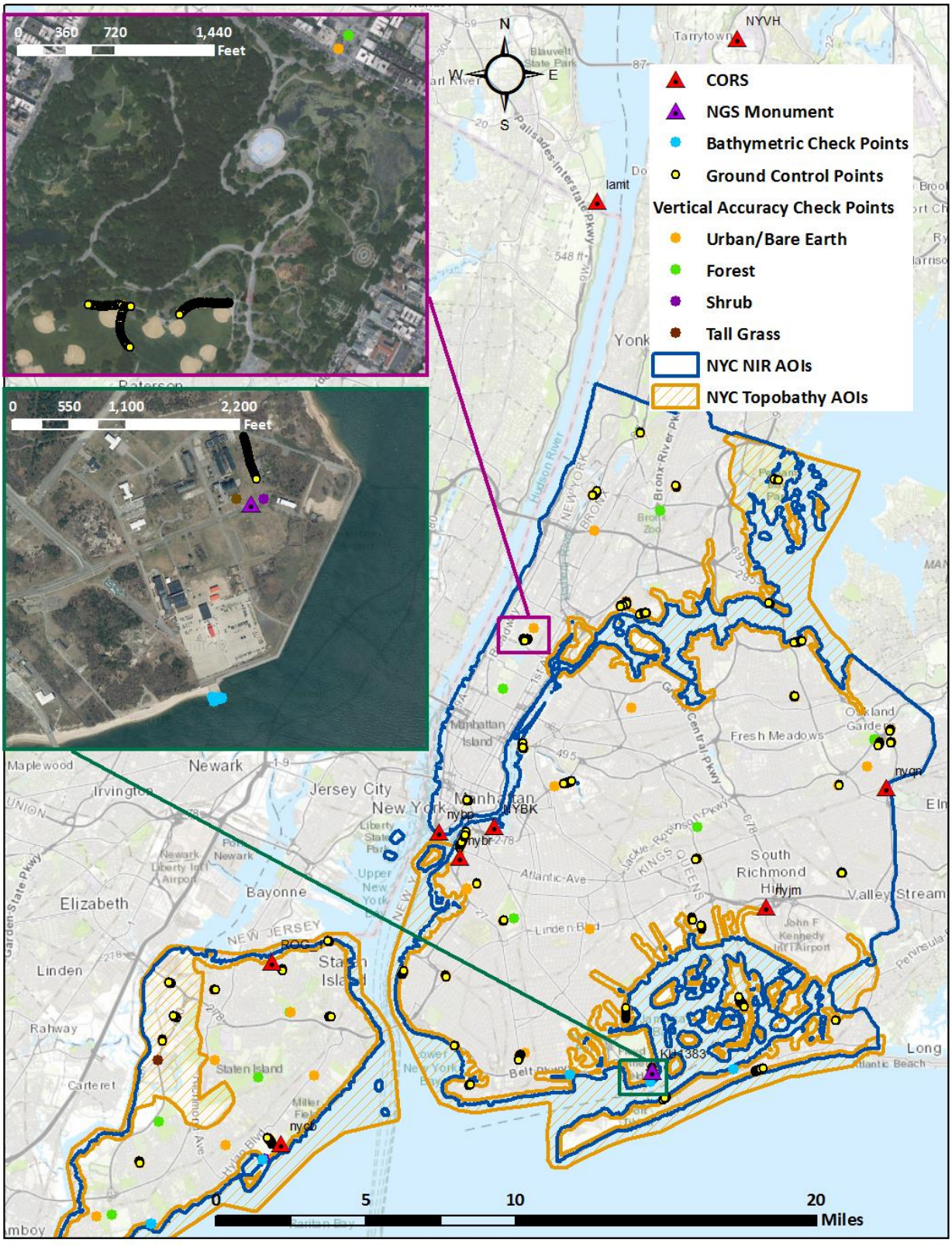

Figure 2: Ground survey location map

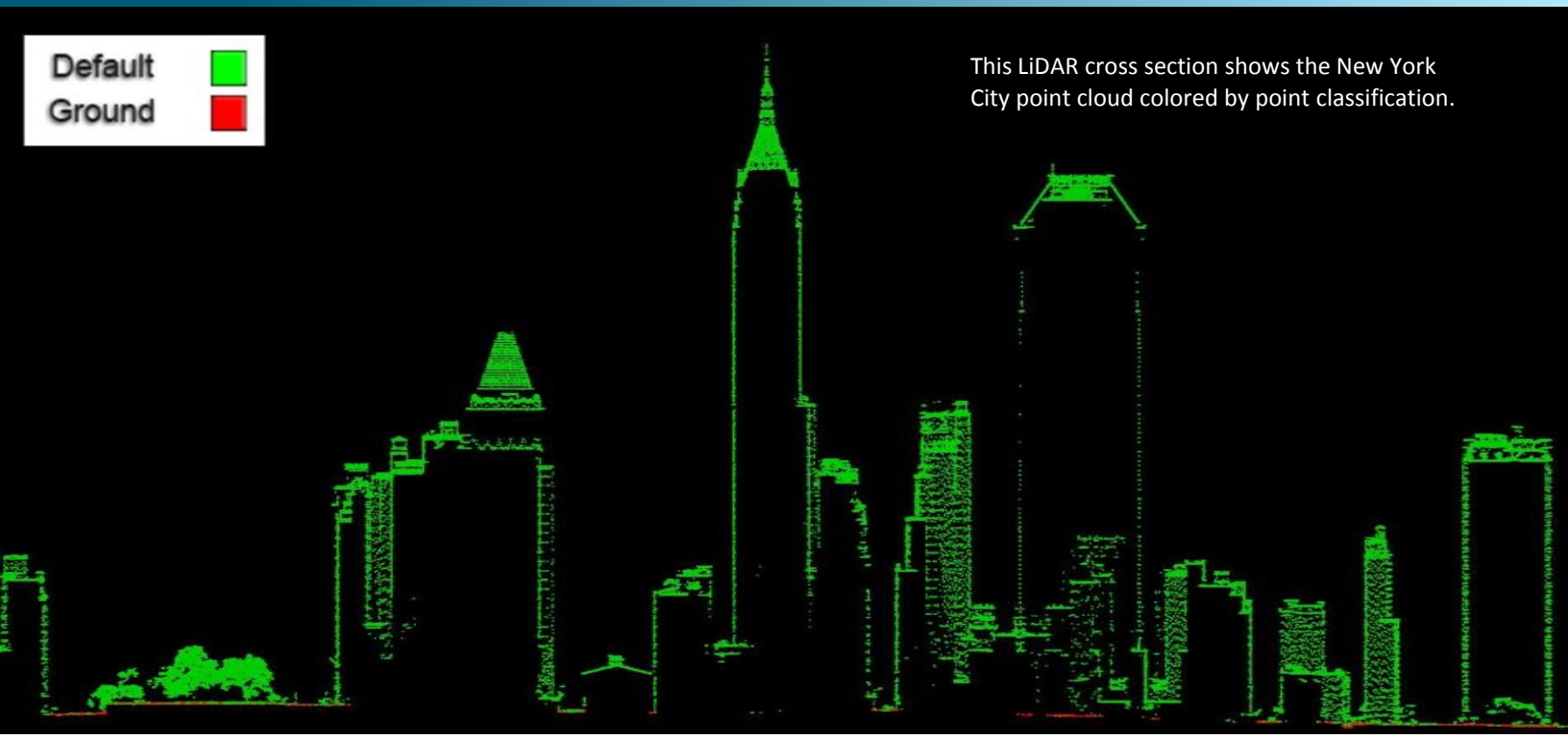

This LiDAR cross section shows the New York City point cloud colored by point classification.

Topographic and Topobathymetric LiDAR Data

Upon completion of data acquisition, QSI processing staff initiated a suite of automated and manual techniques to process the data into the requested deliverables. Processing tasks included GPS control computations, smoothed best estimate trajectory (SBET) calculations, kinematic corrections, calculation of laser point position, sensor and data calibration for optimal relative and absolute accuracy, and LiDAR point classification (Table 8).

For the topobathymetric AOI, Riegl's RiProcess software was used to facilitate bathymetric return processing. Once bathymetric points were differentiated, they were spatially corrected for refraction through the water column based on the angle of incidence of the laser. QSI refracted water column points using QSI's proprietary LAS processing software, LAS Monkey. The resulting point cloud data were classified using both manual and automated techniques. Processing methodologies were tailored for the landscape. Brief descriptions of these tasks are shown in Table 9.

Table 8: ASPRS LAS classification standards applied to the New York City Topographic and Topobathymetric LiDAR dataset

Classification Number	Classification Name	Classification Description	AOI
1	Default/Unclassified	Laser returns that are not included in the ground class, composed of vegetation and anthropogenic features	Topographic and Topobathymetric
1WO	Default/Unclassified – Withheld Overlap	Laser returns that are deemed not necessary to form a complete single, non-overlapped, gap free coverage with respect to adjacent swaths	
2	Ground	Laser returns that are determined to be ground using automated and manual cleaning algorithms	
7W	Noise - Withheld	Laser returns that are often associated with birds, scattering from reflective surfaces, or artificial points below the ground surface	
9	Water	Laser returns that are determined to be water using automated and manual cleaning algorithms	
17	Bridge	Bridge decks	
25	Subway Stairs	Subway Stairs	
40	Bathymetric Bottom	Refracted Riegl sensor returns that fall within the water's edge breakline which characterize the submerged topography.	Topobathymetric Only
41	Water Surface	Green laser returns that are determined to be water surface points using automated and manual cleaning algorithms.	
45	Water Column	Refracted Riegl sensor returns that are determined to be water using automated and manual cleaning algorithms.	

Table 9: LiDAR processing workflow

LiDAR Processing Step	Software Used
Resolve kinematic corrections for aircraft position data using kinematic aircraft GPS and static ground GPS data. Develop a smoothed best estimate of trajectory (SBET) file that blends post-processed aircraft position with sensor head position and attitude recorded throughout the survey.	Waypoint Inertial Explorer v.8.7 POSPac MMS v.8.0
Calculate laser point position by associating SBET position to each laser point return time, scan angle, intensity, etc. Create raw laser point cloud data for the entire survey in *.las (ASPRS v. 1.4) format. Convert data to orthometric elevations by applying a geoid correction.	RiProcess v1.8.2 Waypoint Inertial Explorer v.8.6 Leica Cloudpro v. 1.2.2 TerraMatch v.17
Import raw laser points into manageable blocks to perform manual relative accuracy calibration and filter erroneous points. Classify ground points for individual flight lines.	TerraScan v.17
Using ground classified points per each flight line, test the relative accuracy. Perform automated line-to-line calibrations for system attitude parameters (pitch, roll, heading), mirror flex (scale) and GPS/IMU drift. Calculate calibrations on ground classified points from paired flight lines and apply results to all points in a flight line. Use every flight line for relative accuracy calibration.	TerraMatch v.17 RiProcess v1.8.2
Apply refraction correction to all subsurface returns.	LAS Monkey 2.3 (QSI proprietary software)
Classify resulting data to ground and other client designated ASPRS classifications (Table 8). Assess statistical absolute accuracy via direct comparisons of ground classified points to ground control survey data.	TerraScan v.17 TerraModeler v.17
Generate bare earth models as triangulated surfaces. Generate highest hit models as a surface expression of all classified points. Export all surface models as GeoTIFF format at a 1 foot pixel resolution.	TerraScan v.17 TerraModeler v.17 ArcMap v. 10.2.2
Export intensity images as GeoTIFFs at a 1 foot pixel resolution.	ArcMap v. 10.3.1 Las Product Creator 3.0 (QSI proprietary software)

Boardwalk Removal

After deliberating with NYC, it was decided that wooden and concrete boardwalks which are known to be on pylons and separation is clearly visible, were to be removed from the bare earth models. Triangulation due to interpolation will be seen in these areas. (Figure 3)

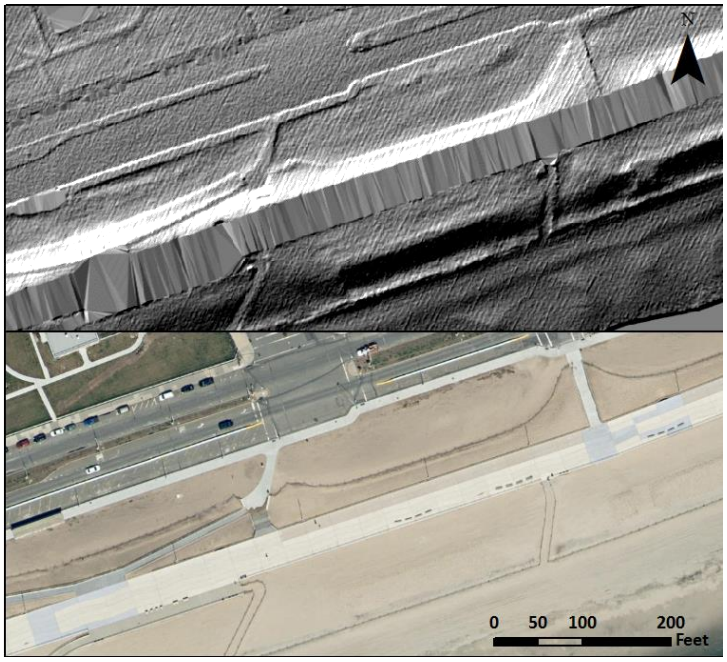

Figure 3: Boardwalk Removal

Bathymetric Refraction

The water surface models used for refraction are generated using elevation information derived from the NIR and Green channels to inform where the water surface level is located, and then water surface points are classified for both the forward and reverse look directions. Points are filtered and edited to obtain the most accurate representation of the water surface and are used to create a water surface model for each flight line and look direction. Water surface classification and modeling is processed on each flight line to accommodate water level changes due to tide and temporal changes in water surface. Each look direction (forward and reverse) are modeled separately to correctly model short duration time dependent surface changes (e.g. waves) that change between the times that each look direction records a unique location. The water surface model created is raster based with an associated surface normal vector to obtain the most accurate angle of incidence during refraction. Once an accurate water surface model is created, the refraction processing is done using LasMonkey, QSI's proprietary software.

Splicing the Topographic and Bathymetric Data

The Topobathymetric AOI was created using data from both the Topographic NIR LiDAR flightlines and the topobathymetric Green LiDAR flightlines. Water's edge breaklines were used to delineate the area where bathymetric (green) data would be inserted (spliced) into the NIR topographic dataset. Using the water's edge breakline as the delineator, NIR data falling within the breaklines was removed, and replaced with green sensor data. Because the NIR and green LiDAR flights took place between May of

2017, and July of 2017, temporal differences between datasets did necessitate additional interpretation and data manipulation at the splicing boundary (Figure 4 and Figure 5). Steps were taken to minimize the differences and provide the smoothest bare earth models as possible. The main goal was to preserve data that was under water at the time of the NIR acquisition but exposed as dry land or valid bathymetric bottom during the topobathymetric acquisition.

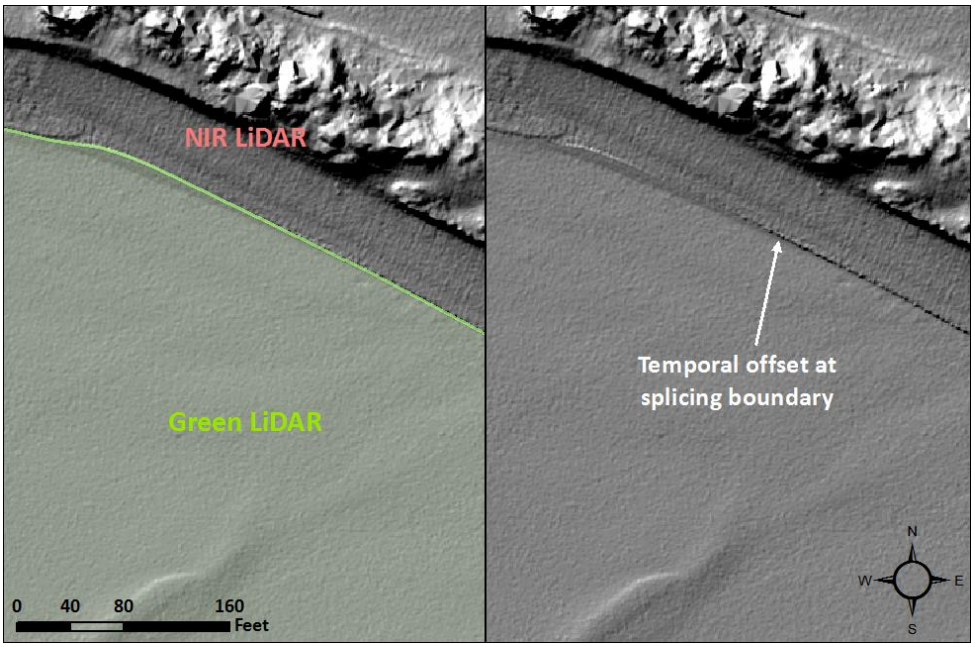

Figure 4: This image of the topobathymetric DEM labels the locations of the Green LiDAR and NIR LiDAR and provides an example of temporal offsets that may be seen

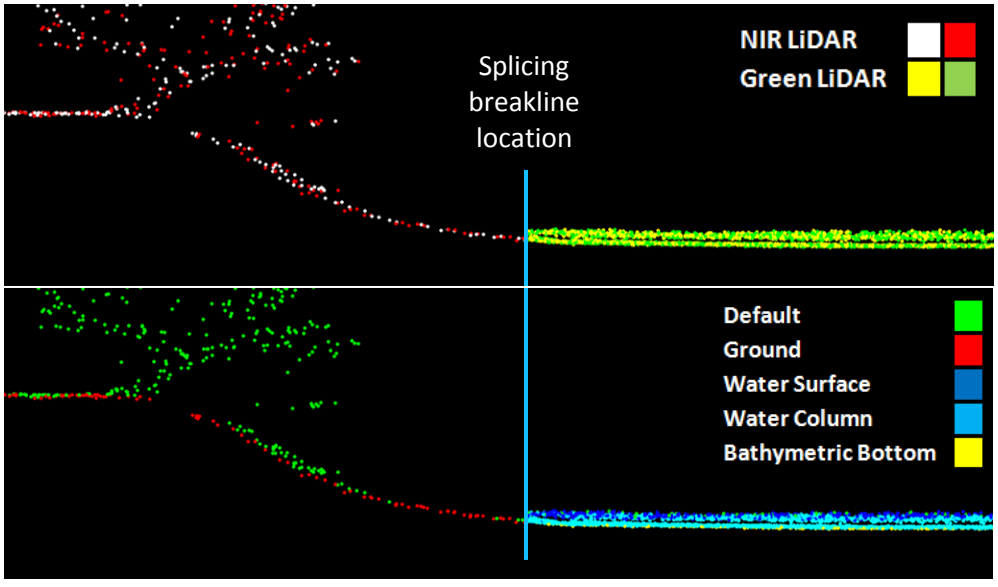

Figure 5: This image shows a three-foot cross-section of spliced NIR and Green LiDAR within the point cloud. The top image is colored by scanner (NIR or Green) and the bottom image is colored by point classification

Feature Extraction

Hydroflattening and Water's Edge Breaklines

The tidal areas surrounding the New York City LiDAR Topographic AOI and other water bodies within the project area were flattened to a consistent water level. Bodies of water that were flattened include lakes and other closed water bodies with a surface area greater than 0.25 acres, all streams and rivers that are nominally wider than 20 feet, all tidal waters bordering the project, and select smaller bodies of water as feasible. The hydroflattening process eliminates artifacts in the digital terrain model caused by both increased variability in ranges or dropouts in laser returns due to the low reflectivity of water.

Hydroflattening of closed water bodies was performed through a combination of automated and manual detection and adjustment techniques designed to identify water boundaries and water levels. Boundary polygons were developed using an algorithm which weights LiDAR-derived slopes, intensities, and return densities to detect the water's edge. The water edges were then manually reviewed and edited as necessary.

Once polygons were developed the initial ground classified points falling within water polygons were reclassified as water points to omit them from the final ground model. Elevations were then obtained from the filtered LiDAR returns to create the final breaklines. Lakes were assigned a consistent elevation for an entire polygon while rivers were assigned consistent elevations on opposing banks and smoothed to ensure downstream flow through the entire river channel.

Water boundary breaklines were then incorporated into the hydroflattened DEM by enforcing triangle edges (adjacent to the breakline) to the elevation values of the breakline. This implementation corrected interpolation along the hard edge. Water surfaces were obtained from a TIN of the 3D water edge breaklines resulting in the final hydroflattened model (Figure 6).

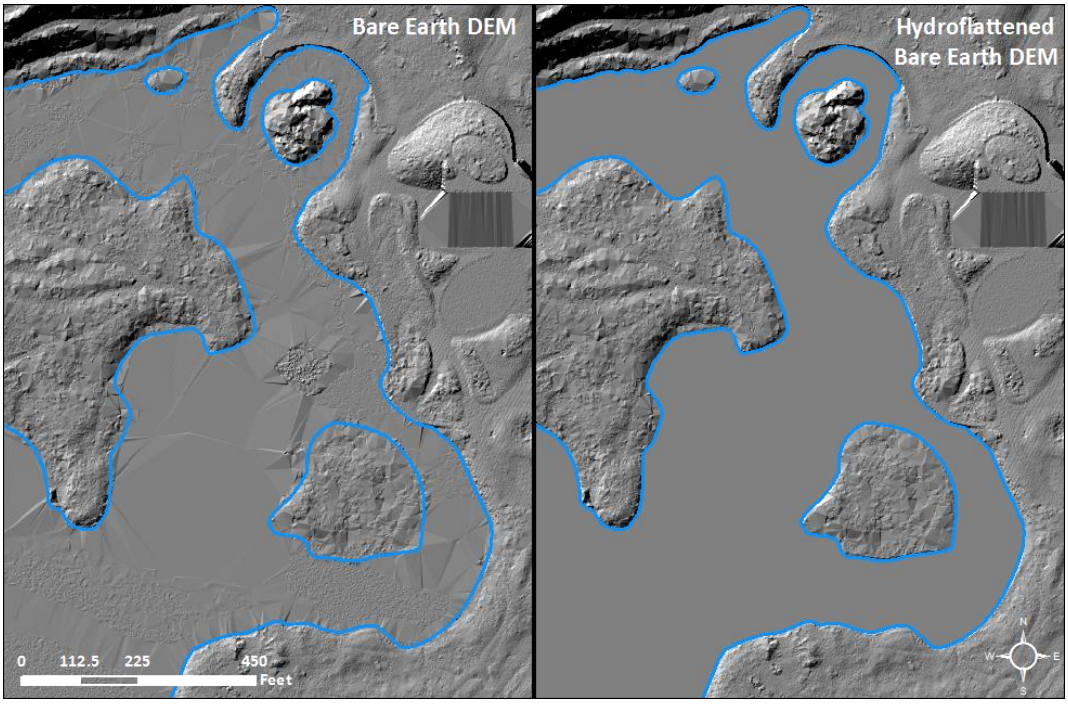

Figure 6: Example of hydroflattening in the New York City Topographic LiDAR dataset

Hydro-enforcement

Hydro-enforced DEMs for the New York City Topographic LiDAR site were generated from the LiDAR-derived bare earth DEMs using ArcHydro 2.0. An initial network was generated by filling all sinks (depressions) in the model and identifying all paths of flow with an accumulation threshold of at least 2.5 acres. The initial stream network was inspected for artificial obstructions to the flow (e.g., culverts beneath roads that allow flow but are not reflected in the normal bare earth model). Hydro-enforcement breaklines were then incorporated into the bare earth model at obstruction locations to enforce the appropriate flow path (Figure 7). Two hydro-enforced DEMs were produced, one with the enforcements burned into the DEM but with no sinks filled and one with ArcHydro run on the enforced DEMs, filling all sinks.

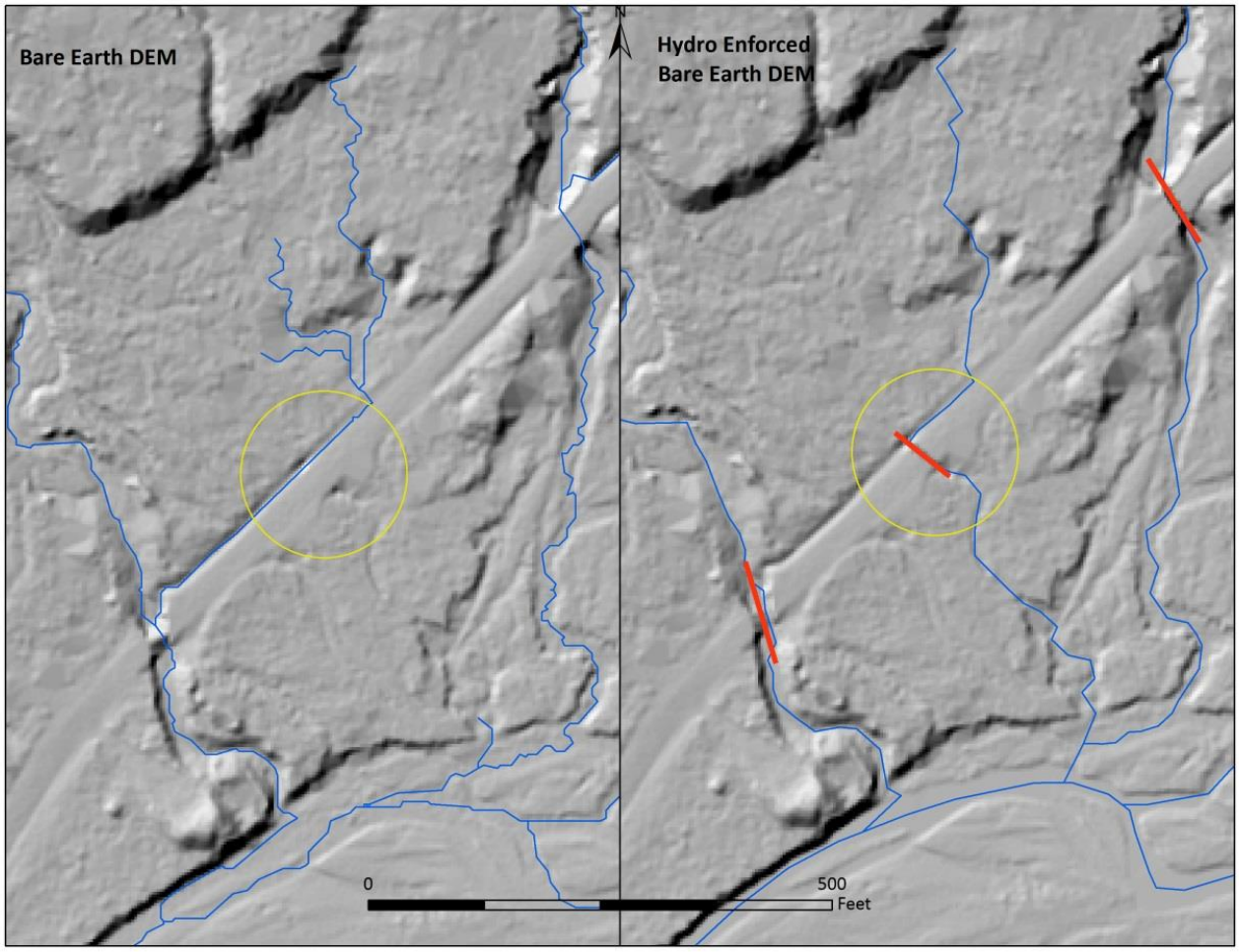

Figure 7: An example of an ArcHydro generated stream network displayed over a bare earth DEM and a hydro-enforced bare earth DEM. The red lines indicate areas on the DEM that were 'enforced' to correct erroneous flow paths.

Topobathymetric LiDAR-Derived Products

Because hydrographic laser scanners penetrate the water surface to map submerged topography, this affects how the data should be processed and presented in derived products from the Topobathymetric AOI point cloud. The following discusses certain derived products that vary from the traditional (NIR) specification and delivery format.

Topobathymetric DEMs

Bathymetric bottom returns can be limited by depth, water clarity, and bottom surface reflectivity. Water clarity and turbidity affects the depth penetration capability of the green wavelength laser with returning laser energy diminishing by scattering throughout the water column. Additionally, the bottom surface must be reflective enough to return remaining laser energy back to the sensor at a detectable level. Although the predicted depth penetration range of the Riegl VQ-880-G sensor is 1.5 Secchi depths on brightly reflective surfaces, it is not unexpected to have no bathymetric bottom returns in turbid or non-reflective areas.

As a result, creating digital elevation models (DEMs) presents a challenge with respect to interpolation of areas with no returns. Traditional DEMs are “unclipped”, meaning areas lacking ground returns are interpolated from neighboring ground returns (or breaklines in the case of hydro-flattening), with the assumption that the interpolation is close to reality. In bathymetric modeling, these assumptions are prone to error because a lack of bathymetric returns can indicate a change in elevation that the laser can no longer map due to increased depths. The resulting void areas may suggest greater depths, rather than similar elevations from neighboring bathymetric bottom returns. Therefore, QSI created a water polygon with bathymetric coverage to delineate areas with successfully mapped bathymetry. This shapefile was used to control the extent of the delivered clipped topobathymetric model to avoid false triangulation (interpolation from TIN’ing) across areas in the water with no bathymetric returns.

Intensity Images

For the New York City Topographic and Topobathymetric LiDAR project, QSI created traditional NIR LiDAR intensity images from first return intensity information for the Topographic only AOI. Due to the different collection wavelengths of the ALS80 (1064 nm) and the VQ-880 (532 nm) the topobathymetric AOI required additional filtering. The green laser portion of these intensity images (located within the water’s edge breaklines) were created using water column and bathymetric bottom points in order to display more detail in intensity values in the sub water surface features of interest. The terrestrial portion of the AOI (outside of the water’s edge breaklines) was created in the traditional manner using the NIR first returns. The difference in intensity by sensor/wavelength can be seen in Figure 8.

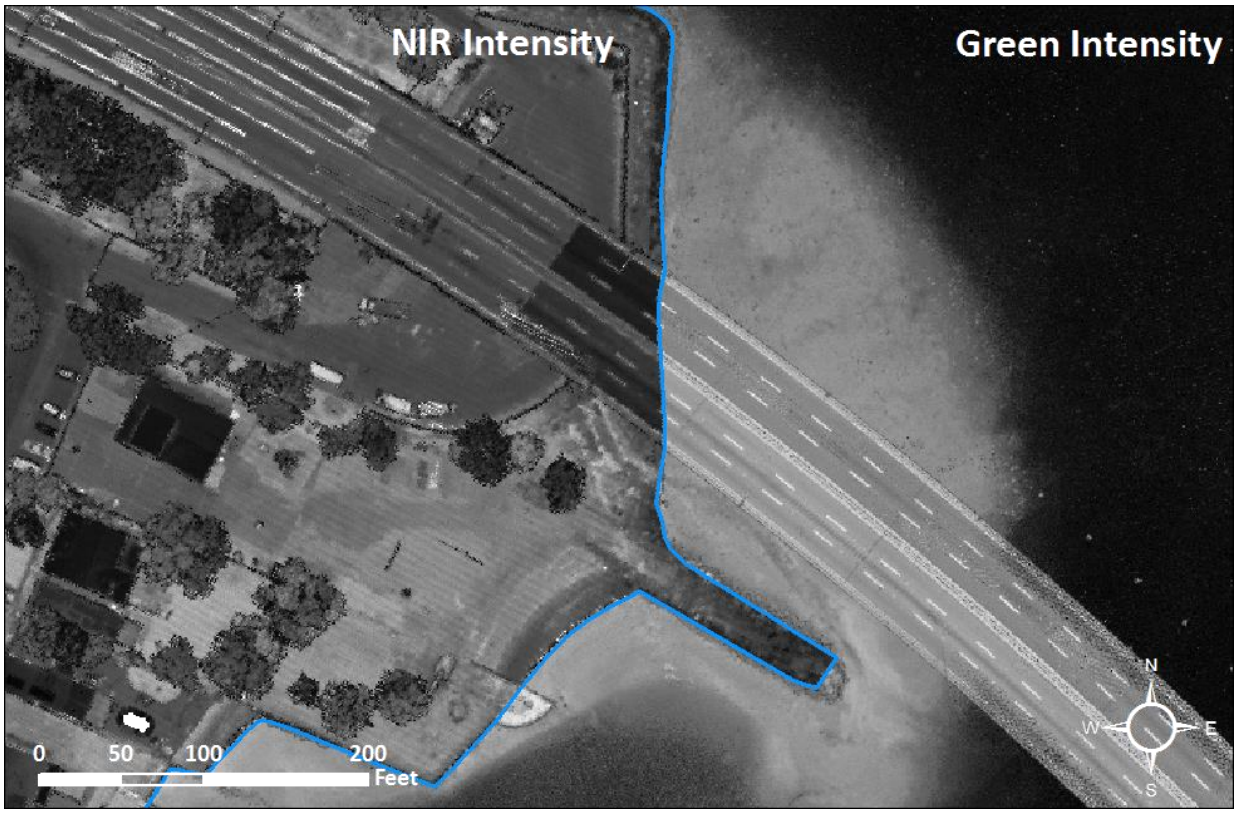

Figure 8: A comparison of Intensity Images from NIR and Green returns in the New York City Topographic and Topobathymetric LiDAR area

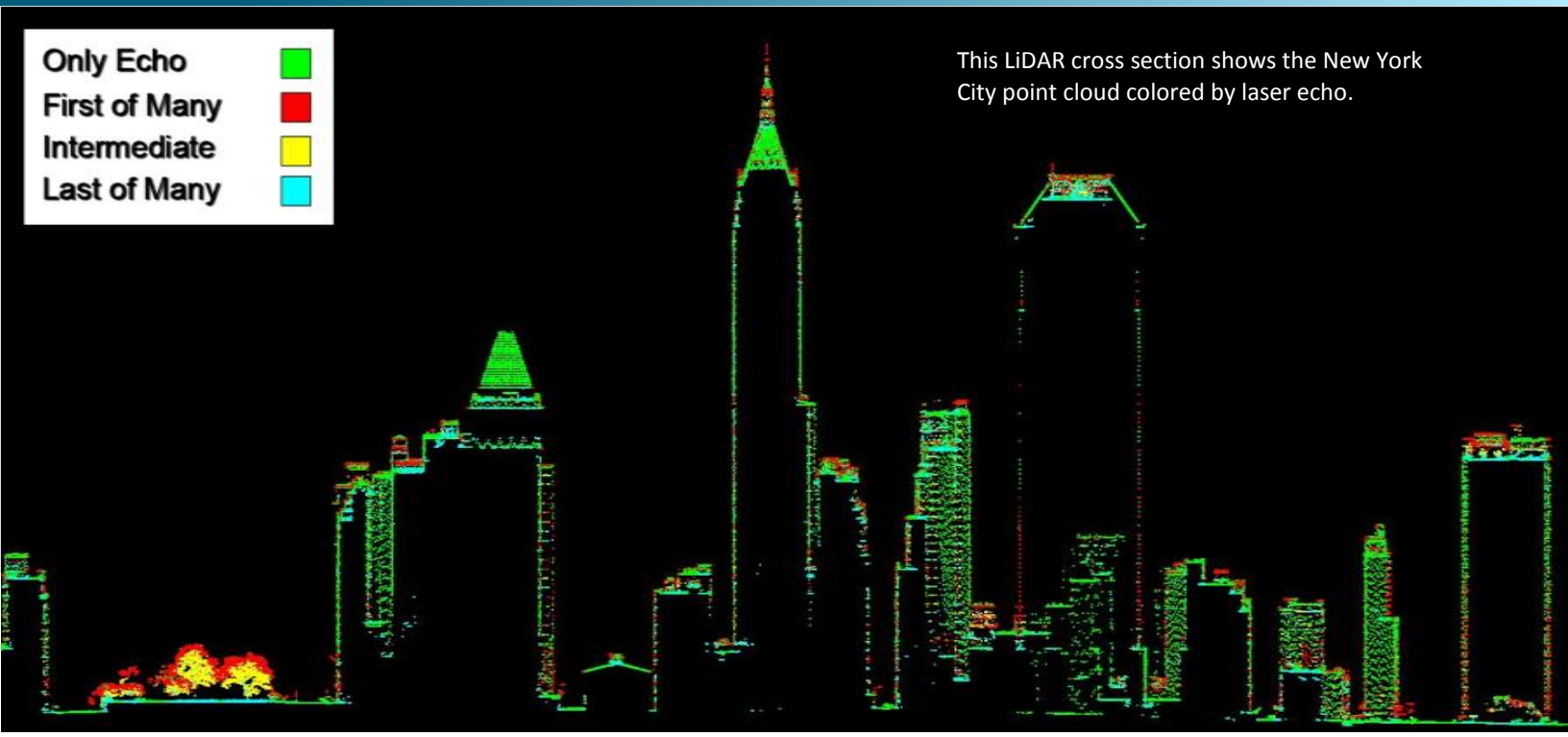

This LiDAR cross section shows the New York City point cloud colored by laser echo.

Bathymetric LiDAR

An underlying principle for collecting hydrographic LiDAR data is to survey near-shore areas that can be difficult to collect with other methods, such as multi-beam sonar, particularly over large areas. In order to determine the capability and effectiveness of the bathymetric LiDAR, QSI considered bathymetric return density and spatial accuracy.

Mapped Bathymetry

Within the bathymetric portion of the topobathymetric AOI, a polygon layer was created to delineate areas where bathymetry was successfully mapped. This shapefile was used to control the extent of the delivered clipped topobathymetric model and to avoid false triangulation across areas in the water with no returns. Insufficiently mapped areas were identified by triangulating bathymetric bottom points with an edge length maximum of 15.2 feet. This ensured all areas of no returns (> 100 ft^2), were identified as data voids.

LiDAR Point Density

First Return Point Density

The acquisition parameters were designed to acquire an average first-return density of 8 points/m^2. First return density describes the density of pulses emitted from the laser that return at least one echo to the system. Multiple returns from a single pulse were not considered in first return density analysis. Some types of surfaces (e.g., breaks in terrain, water and steep slopes) may have returned fewer pulses than originally emitted by the laser.

First returns typically reflect off the highest feature on the landscape within the footprint of the pulse. In forested or urban areas the highest feature could be a tree, building or power line, while in areas of unobstructed ground, the first return will be the only echo and represents the bare earth surface.

The average first-return density for the Topographic AOI was 1.00 points/ft^2 (10.75 points/m^2), while the average first-return density of the Topobathymetric AOI was 1.42 points/ft^2 (15.24 points/m^2) (Table 11). The statistical and spatial distributions of all first return densities per 100 m x 100 m cell are portrayed in Figure 9 through Figure 11.

Table 10: Average First Return Densities

New York City Topographic AOI Densities	
Density Type	**Point Density**
Topographic AOI First Returns	1.00 points/ft² (10.75 points/m²)
Topobathymetric AOI First Returns	1.42 points/ft² (15.24 points/m²)

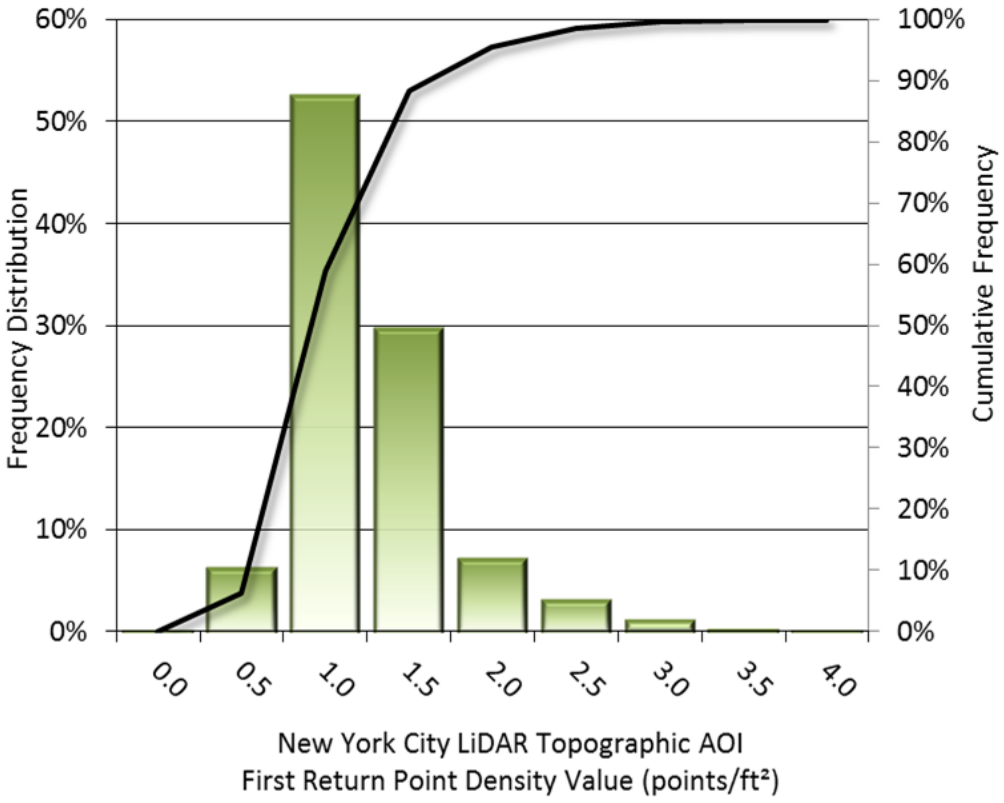

Figure 9: Frequency distribution of LiDAR first return densities of the Topographic AOI, per 100 x 100 m cell

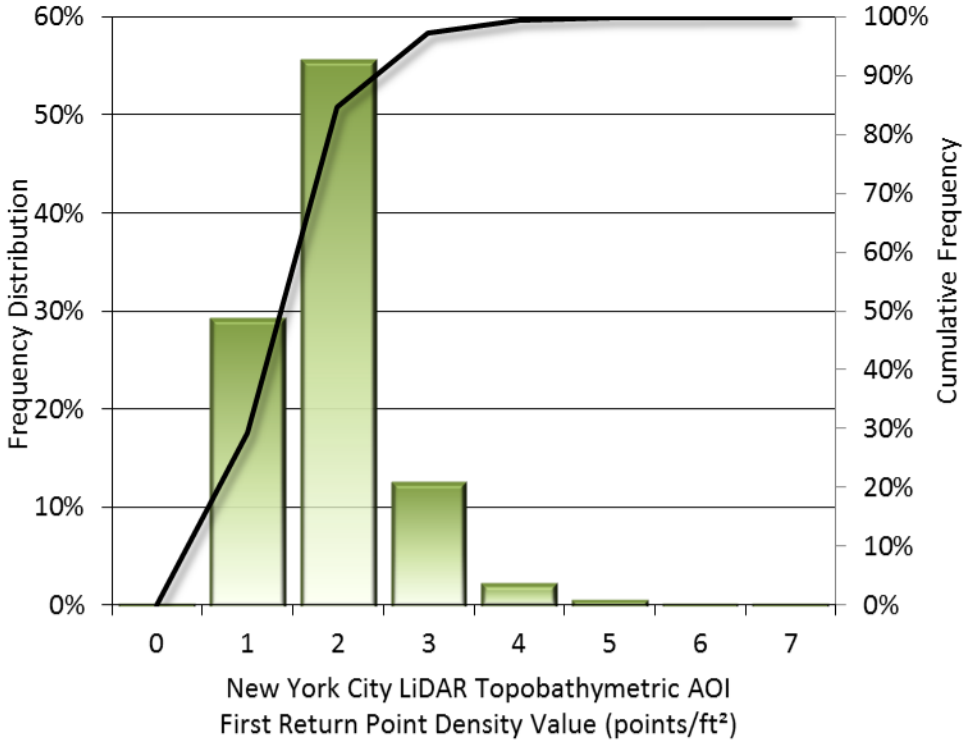

Figure 10: Frequency distribution of LiDAR first return densities of the Topobathymetric AOI, per 100 x 100 m cell

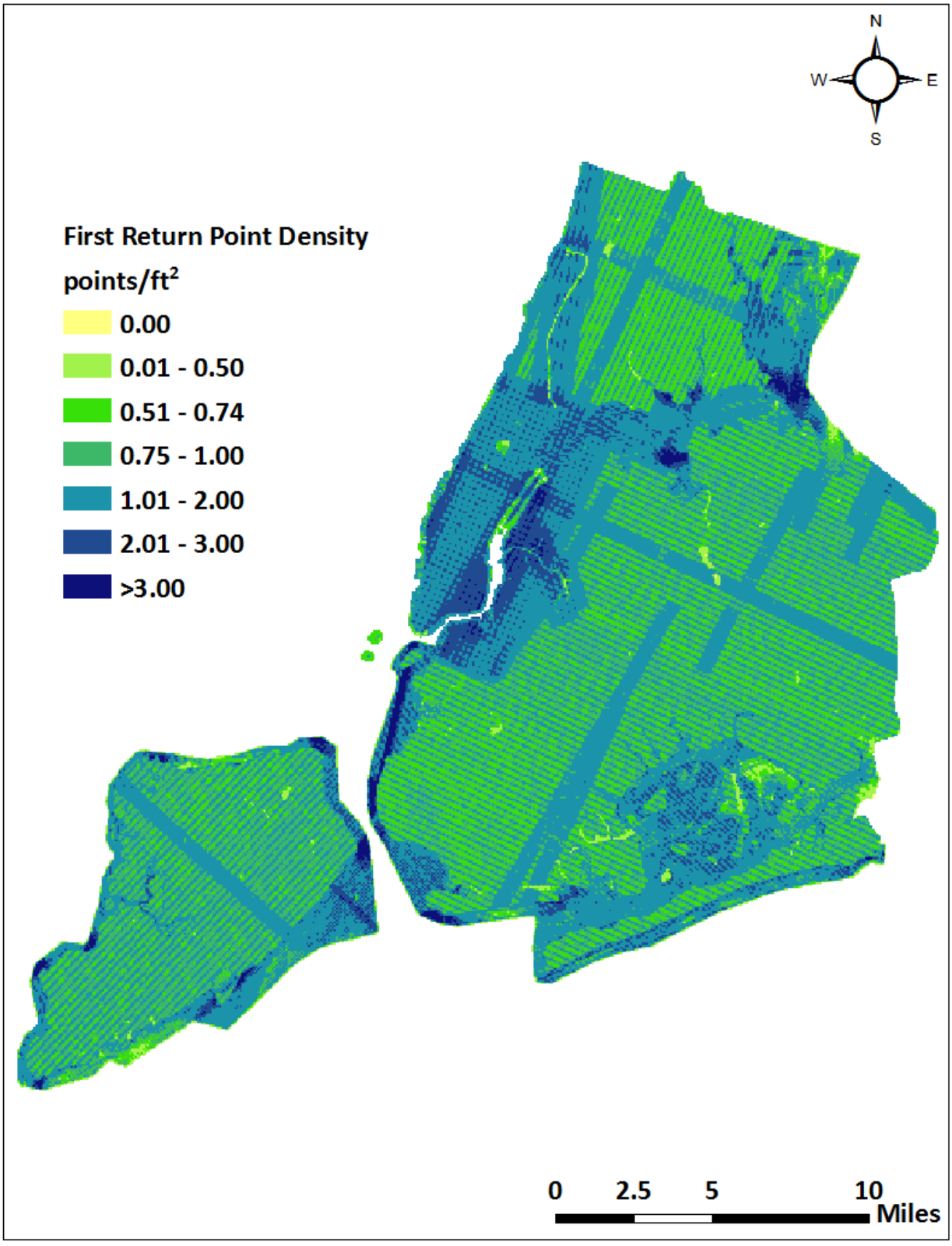

Figure 11: First return density map for the New York City Topographic and Topobathymetric LiDAR sites (100 m x 100 m cells)

Ground and Bathymetric Bottom Classified Point Densities

The density of ground classified LiDAR returns and bathymetric bottom returns were also analyzed for this project. Terrain character, land cover, and ground surface reflectivity all influenced the density of ground surface returns. In vegetated areas, fewer pulses may have penetrated the canopy, resulting in lower ground density. Similarly, the density of bathymetric bottom returns was influenced by turbidity, depth, and bottom surface reflectivity. In turbid areas, fewer pulses may have penetrated the water surface, resulting in lower bathymetric density.

The average ground classified return density of LiDAR data for the Topographic AOI was 0.38 points/ft^2 (4.13 points/m^2) (Table 11). For the Topobathymetric AOI, the combined ground and bathymetric bottom classified return density was 0.38 points/ft^2 (4.07 points/m^2) (Table 11). The statistical and spatial distributions ground classified and bathymetric bottom return densities per 100 m x 100 m cell are portrayed in Figure 12 through Figure 14.

Additionally, for the Topobathymetric LiDAR AOI, density values of only bathymetric bottom returns were calculated for areas containing at least one bathymetric bottom return. Areas lacking bathymetric returns (voids) were not considered in calculating an average density value. Within the successfully mapped area, a bathymetric bottom return density of 0.38 points/ft^2 (4.12 points/m^2) was achieved.

Table 11: Average Ground Classified LiDAR Densities

New York City Ground Classified Densities	
Project Site	**Point Density**
Topographic AOI - Ground Classified Returns	0.38 points/ft² (4.13 points/m²)
Topobathymetric AOI - Bathymetric Bottom and Ground Classified Returns	0.38 points/ft² (4.07 points/m²)
Topobathymetric AOI - Bathymetric Bottom Classified Returns	0.38 points/ft² (4.12 points/m²)

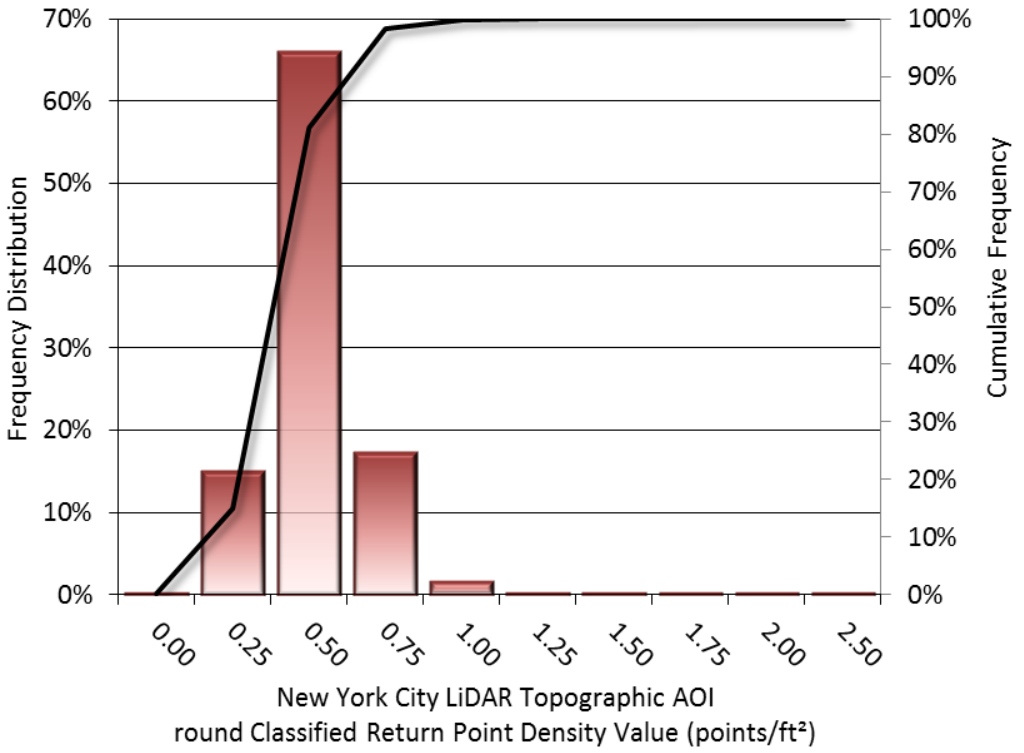

Figure 12: Frequency distribution of ground classified return densities per 100 x 100 m cell

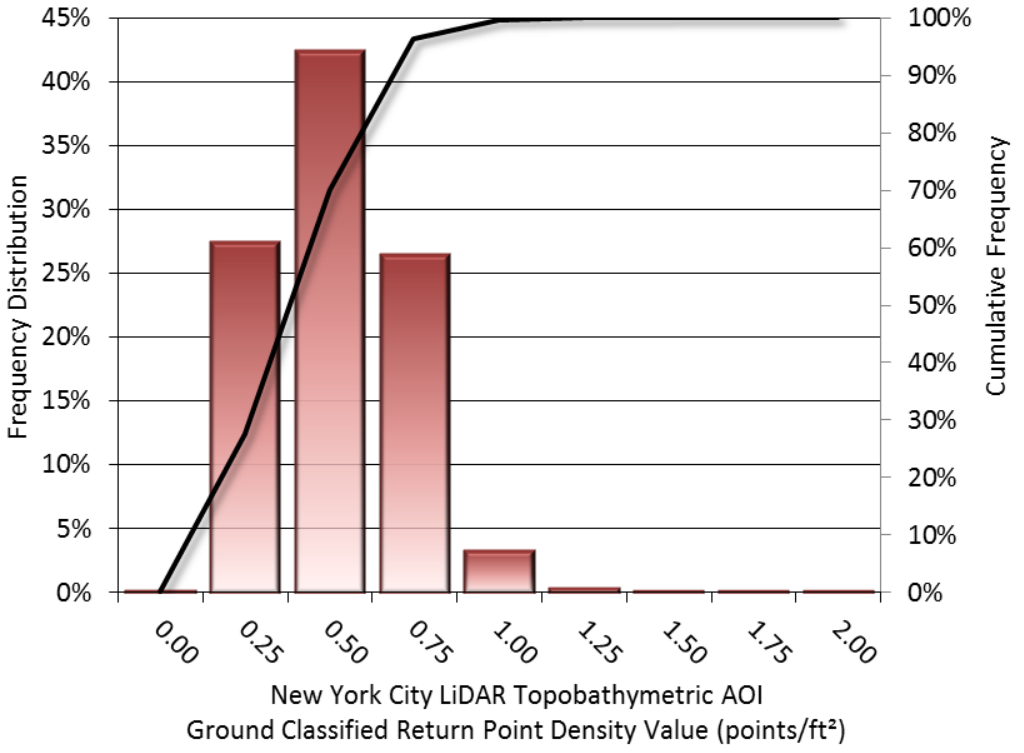

Figure 13: Frequency distribution of ground and bathymetric bottom classified return densities per 100 x 100 m cell

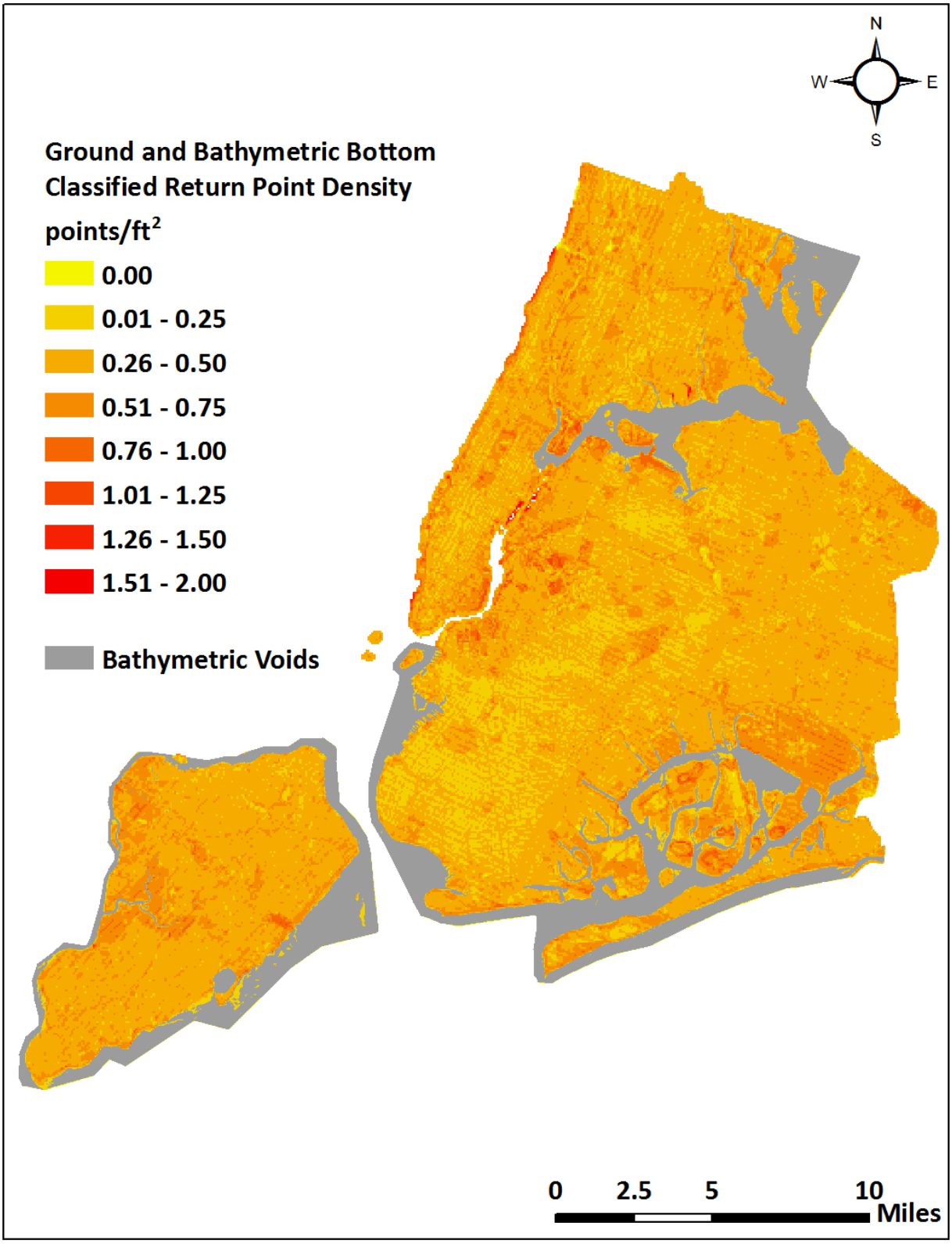

Figure 14: Ground and bathymetric bottom classified return density map for the New York City Topographic and Topobathymetric LiDAR sites (100 m x 100 m cells)

LiDAR Accuracy Assessments

The accuracy of the LiDAR data collection can be described in terms of absolute accuracy (the consistency of the data with external data sources) and relative accuracy (the consistency of the dataset with itself). See Appendix A for further information on sources of error and operational measures used to improve relative accuracy.

LiDAR Non-Vegetated Vertical Accuracy

Absolute accuracy was assessed using Non-vegetated Vertical Accuracy (NVA) reporting designed to meet guidelines presented in the FGDC National Standard for Spatial Data Accuracy[1]. NVA compares known ground quality assurance point data collected on open, bare earth surfaces with level slope (<20°) to the triangulated surface generated by the LiDAR points. NVA is a measure of the accuracy of LiDAR point data in open areas where the LiDAR system has a high probability of measuring the ground surface and is evaluated at the 95% confidence interval (1.96 * RMSE), as shown in Table 12.

The mean and standard deviation (sigma σ) of divergence of the ground surface model from ground check point coordinates are also considered during accuracy assessment. These statistics assume the error for x, y and z is normally distributed, and therefore the skew and kurtosis of distributions are also considered when evaluating error statistics. For the New York City Topographic and Topobathymetric LiDAR survey, 151 ground check points were withheld from the calibration and post-processing of the LiDAR point cloud, resulting in a non-vegetated vertical accuracy of 0.242 feet (0.074 meters), with 95% confidence (Figure 15).

Bathymetric (submerged or along the water's edge) check points were also collected in order to assess the submerged surface vertical accuracy. Assessment of 115 bathymetric check points resulted in a vertical accuracy of 0.208 feet (0.064 meters), evaluated at the 95th percentile (Table 12, Figure 16).

QSI also assessed absolute accuracy using 2,416 ground control points. Although these points were used in the calibration and post-processing of the LiDAR point cloud, they still provide a good indication of the overall accuracy of the LiDAR dataset, and therefore have been provided in Table 12 and Figure 17.

[1] Federal Geographic Data Committee, ASPRS POSITIONAL ACCURACY STANDARDS FOR DIGITAL GEOSPATIAL DATA EDITION 1, Version 1.0, NOVEMBER 2014. http://www.asprs.org/PAD-Division/ASPRS-POSITIONAL-ACCURACY-STANDARDS-FOR-DIGITAL-GEOSPATIAL-DATA.html.

Table 12: Absolute accuracy (NVA) results

Non-Vegetated Vertical Accuracy			
	Ground Check Points	**Submerged Check Points**	**Ground Control Points**
Sample	151 points	115 points	2,416 points
95% Confidence (1.96*RMSE)	0.242 ft 0.074 m	N/A	0.252 ft 0.077 m
95th Percentile	N/A	0.208 ft 0.064 m	N/A
Average	0.024 ft 0.007 m	0.031 ft 0.010 m	0.013 ft 0.004 m
Median	0.023 ft 0.007 m	0.023 ft 0.007 m	0.015 ft 0.005 m
RMSE	0.123 ft 0.038 m	0.114 ft 0.035 m	0.128 ft 0.039 m
Standard Deviation (1σ)	0.121 ft 0.037 m	0.110 ft 0.034 m	0.128 ft 0.039 m

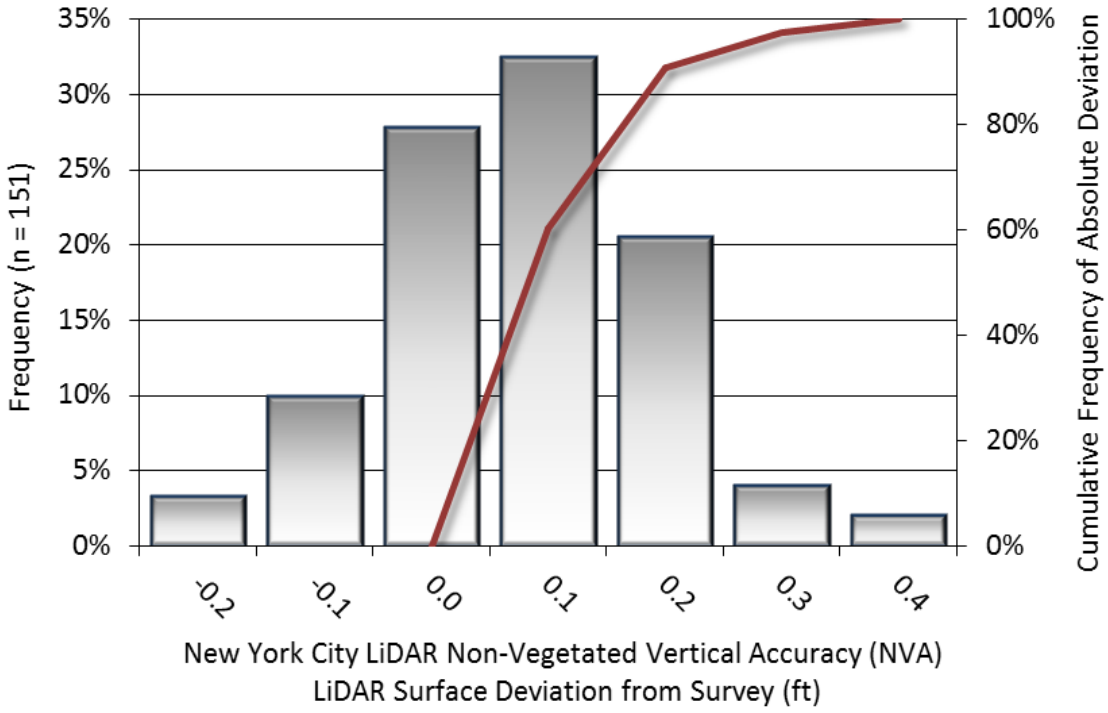

Figure 15: Frequency histogram for LiDAR surface deviation from ground check point values

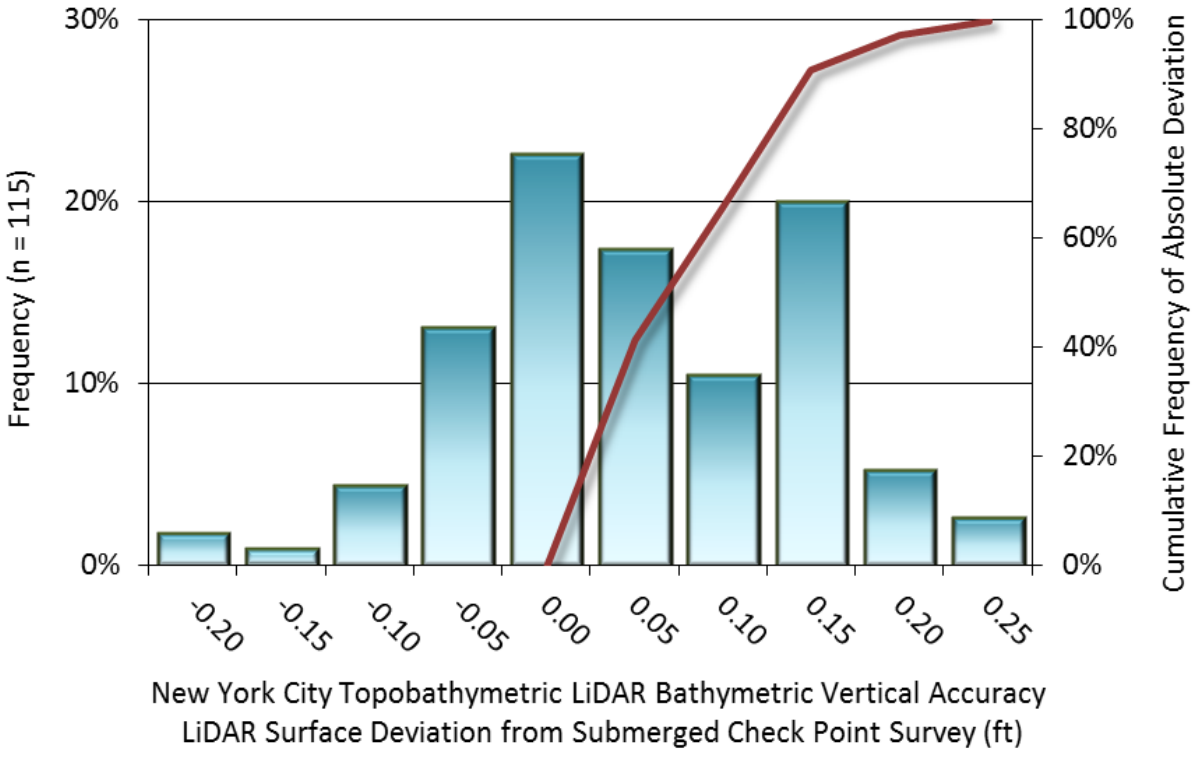

Figure 16: Frequency histogram for LiDAR surface deviation from bathymetric check point values

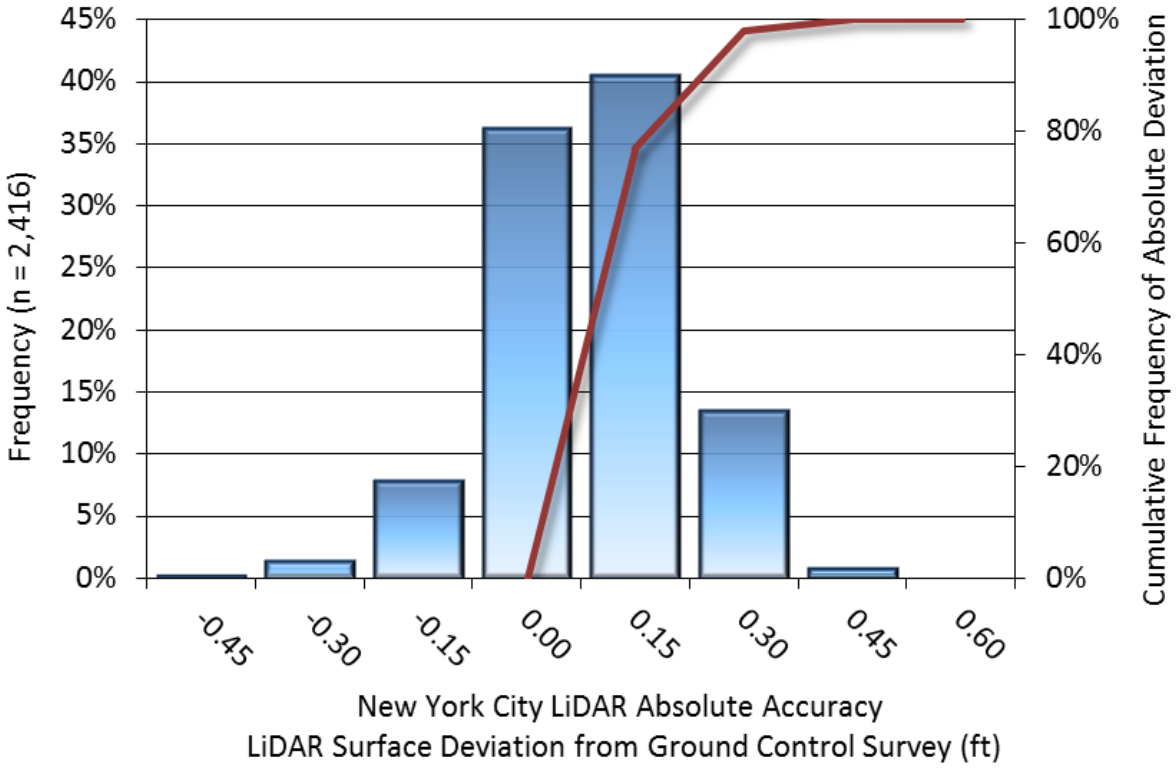

Figure 17: Frequency histogram for LiDAR surface deviation ground control point values

LiDAR Vegetated Vertical Accuracies

QSI also assessed vertical accuracy using Vegetated Vertical Accuracy (VVA) reporting. VVA compares known ground check point data collected over vegetated surfaces using land class descriptions to the triangulated ground surface generated by the ground classified LiDAR points. Evaluation of 18 vegetated check points resulted in a vegetated vertical accuracy of 0.517 feet (0.158 meters), evaluated at the 95th percentile (Table 13, Figure 18).

Table 13: Vegetated Vertical Accuracy for the New York City Topographic and Topobathymetric LiDAR Project

Vegetated Vertical Accuracy (VVA)	
Sample	18 points
Average Dz	0.108 ft 0.033 m
Median	0.049 ft 0.015 m
RMSE	0.252 ft 0.077 m
Standard Deviation (1σ)	0.235 ft 0.072 m
95th Percentile	0.517 ft 0.158 m

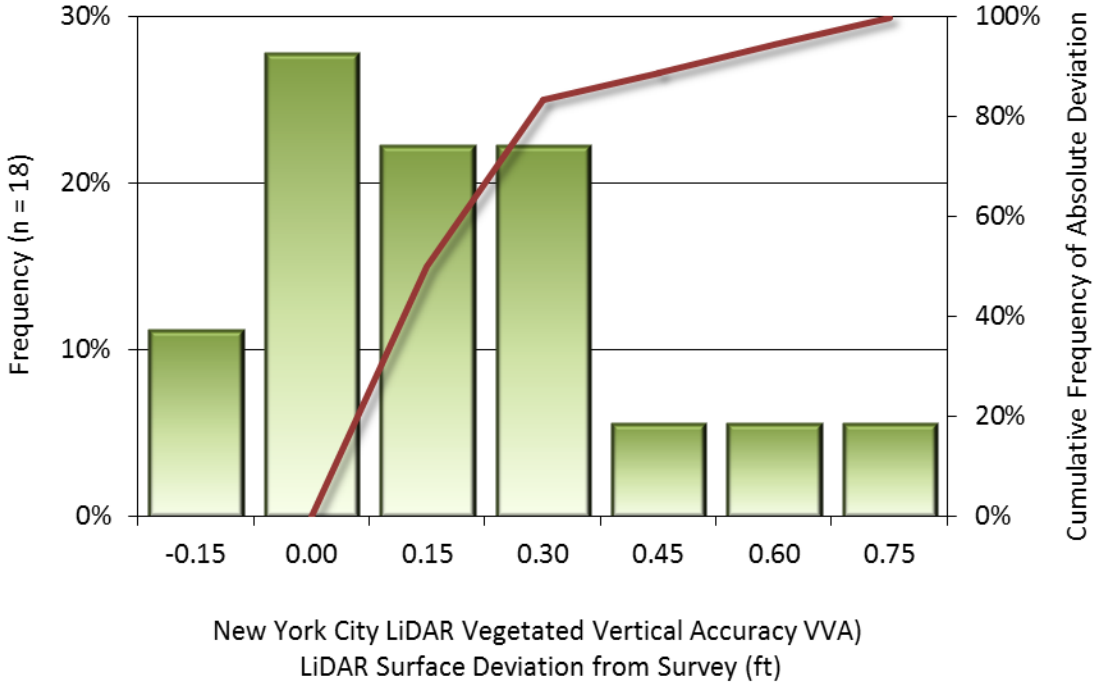

Figure 18: Frequency histogram for LiDAR surface deviation from all land cover class point values (VVA)

LiDAR Relative Vertical Accuracy

Relative vertical accuracy refers to the internal consistency of the data set as a whole: the ability to place an object in the same location given multiple flight lines, GPS conditions, and aircraft attitudes. When the LiDAR system is well calibrated, the swath-to-swath vertical divergence is low (<0.10 meters). The relative vertical accuracy was computed by comparing the ground surface model of each individual flight line with its neighbors in overlapping regions.

The average (mean) line to line relative vertical accuracy for the Topographic AOI was 0.085 feet (0.026 meters) (Table 14, Figure 19) and the average (mean) line to line relative vertical accuracy for the Topobathymetric AOI was 0.089 feet (0.027 meters) (Table 14, Figure 19).

Table 14: Relative accuracy results

Relative Accuracy		
AOI	**Topographic AOI**	**Topobathymetric AOI**
Sample	216 surfaces	541 surfaces
Average	0.085 ft 0.026 m	0.089 ft 0.027 m
Median	0.084 ft 0.026 m	0.085 ft 0.026 m
RMSE	0.085 ft 0.026 m	0.096 ft 0.029 m
Standard Deviation (1σ)	0.008 ft 0.002 m	0.032 ft 0.010 m
1.96σ	0.016 ft 0.005 m	0.062 ft 0.019 m

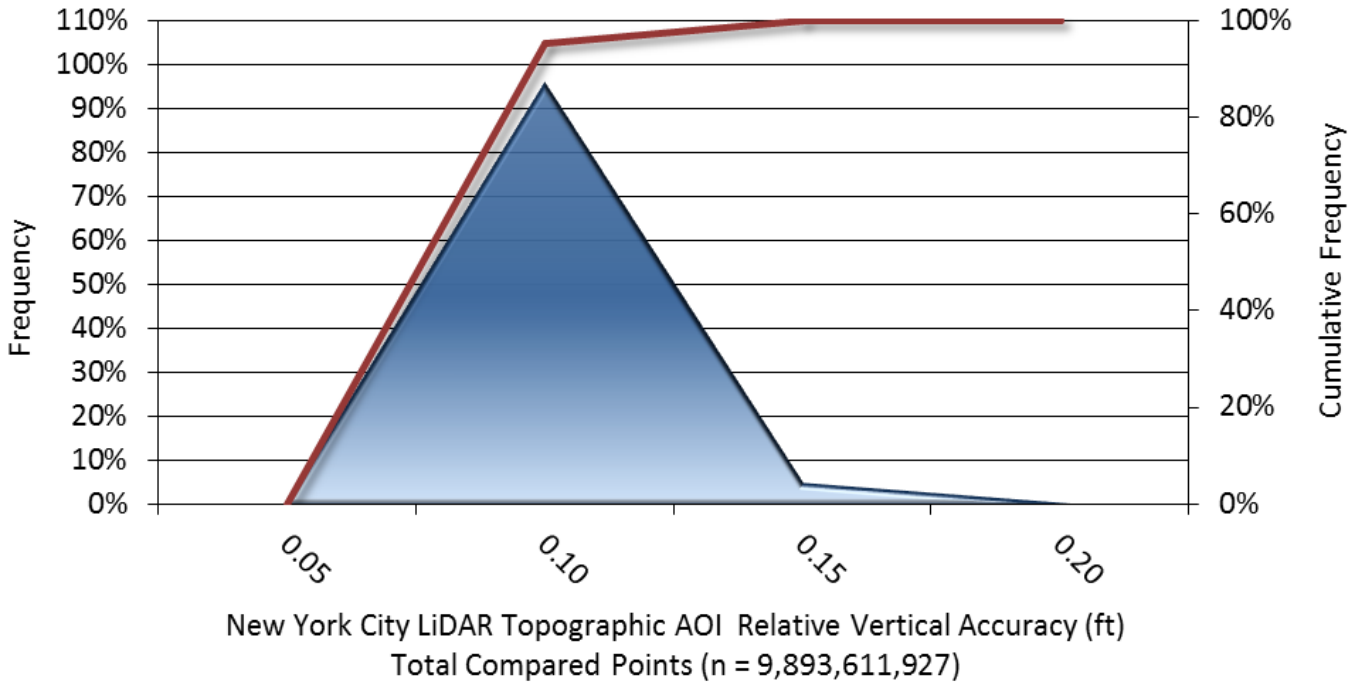

Figure 19: Frequency plot for relative vertical accuracy between flight lines

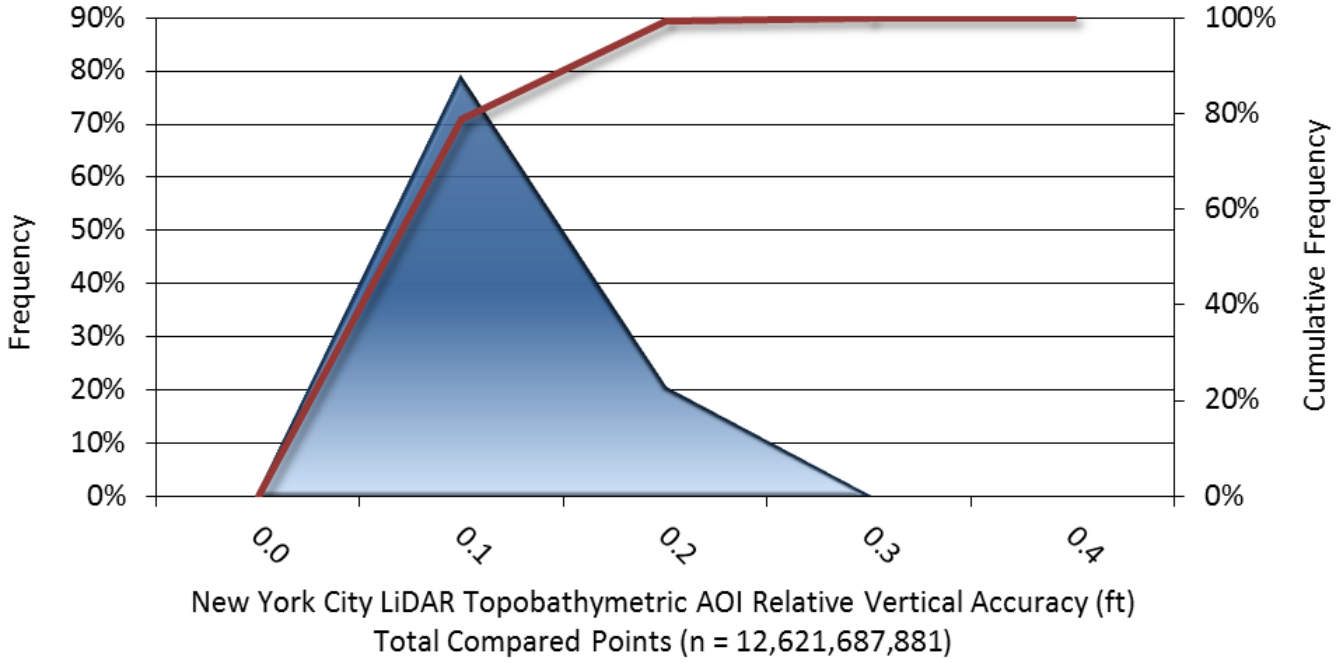

Figure 20: Frequency plot for relative vertical accuracy between flight lines

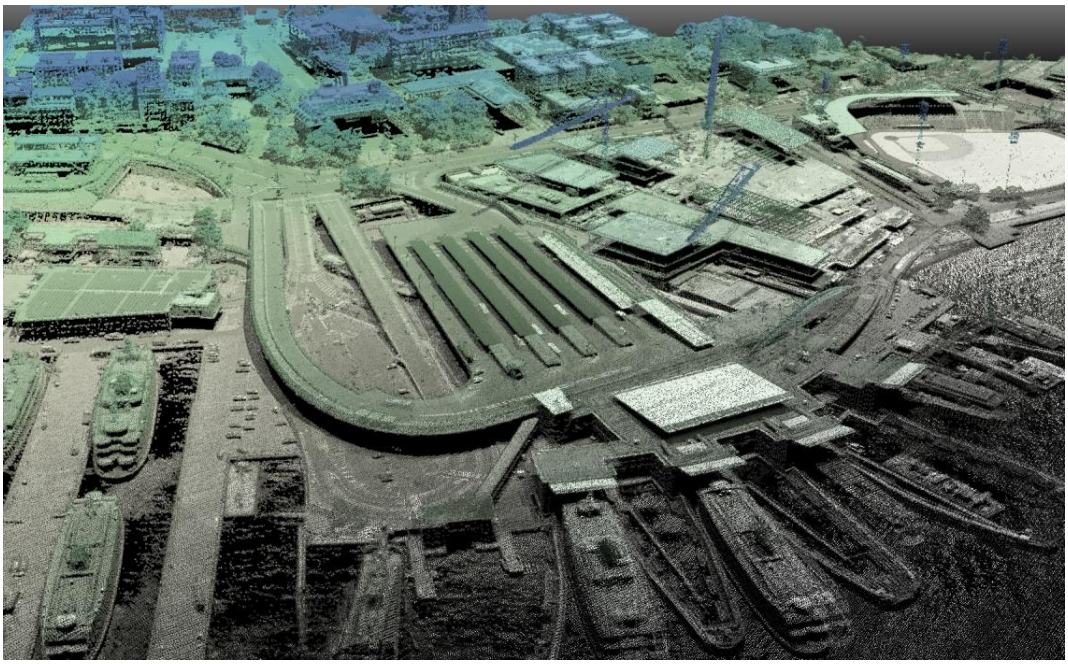

Figure 21: A view of the St. George Ferry Terminal in the New York City LiDAR AOI. The image was created from the LiDAR point cloud and colored by elevation and intensity.

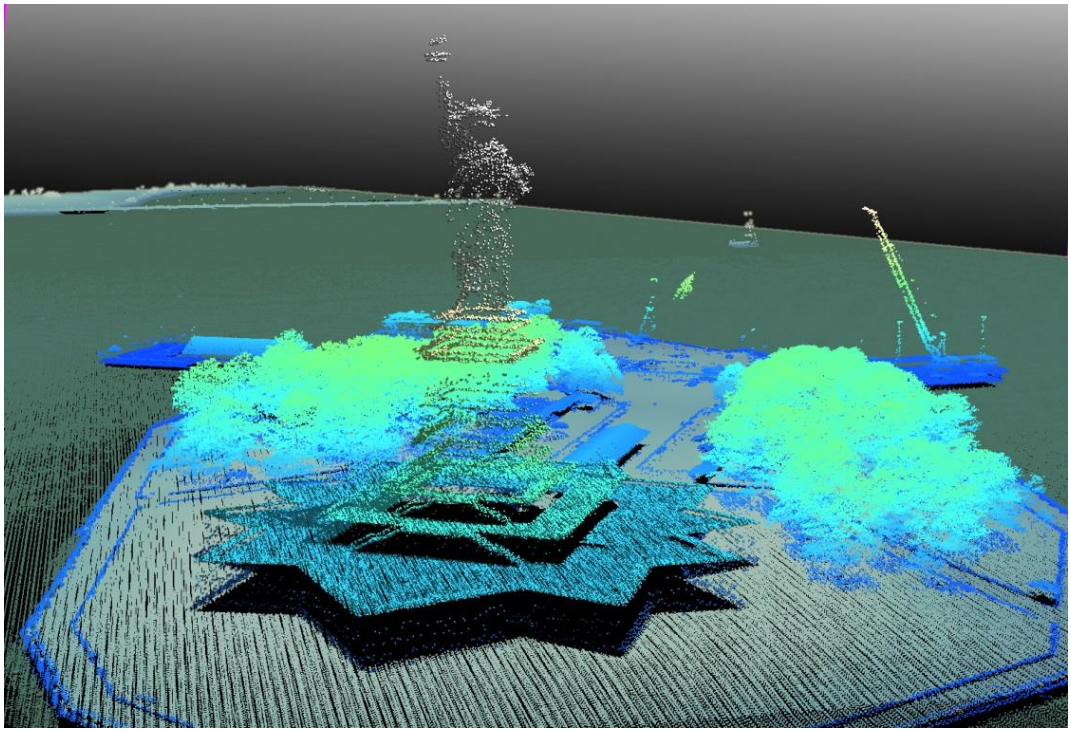

Figure 22: An image of the Statue of Liberty in the New York City, striking northeast. The image was created from the LiDAR point cloud colored by elevation.

Figure 23: A view looking northwest over Central Park in the New York City Topographic and Topobathymetric LiDAR site. The image was created from the LiDAR point cloud

GLOSSARY

1-sigma (σ) Absolute Deviation: Value for which the data are within one standard deviation (approximately 68th percentile) of a normally distributed data set.

1.96 * RMSE Absolute Deviation: Value for which the data are within two standard deviations (approximately 95th percentile) of a normally distributed data set, based on the FGDC standards for Non-vegetated Vertical Accuracy (FVA) reporting.

Accuracy: The statistical comparison between known (surveyed) points and laser points. Typically measured as the standard deviation (sigma σ) and root mean square error (RMSE).

> **Absolute Accuracy:** The vertical accuracy of LiDAR data is described as the mean and standard deviation (sigma σ) of divergence of LiDAR point coordinates from ground survey point coordinates. To provide a sense of the model predictive power of the dataset, the root mean square error (RMSE) for vertical accuracy is also provided. These statistics assume the error distributions for x, y and z are normally distributed, and thus we also consider the skew and kurtosis of distributions when evaluating error statistics.
>
> **Relative Accuracy:** Relative accuracy refers to the internal consistency of the data set; i.e., the ability to place a laser point in the same location over multiple flight lines, GPS conditions and aircraft attitudes. Affected by system attitude offsets, scale and GPS/IMU drift, internal consistency is measured as the divergence between points from different flight lines within an overlapping area. Divergence is most apparent when flight lines are opposing. When the LiDAR system is well calibrated, the line-to-line divergence is low (<10 cm).
>
> **Root Mean Square Error (RMSE):** A statistic used to approximate the difference between real-world points and the LiDAR points. It is calculated by squaring all the values, then taking the average of the squares and taking the square root of the average.

Data Density: A common measure of LiDAR resolution, measured as points per square meter.

Digital Elevation Model (DEM): File or database made from surveyed points, containing elevation points over a contiguous area. Digital terrain models (DTM) and digital surface models (DSM) are types of DEMs. DTMs consist solely of the bare earth surface (ground points), while DSMs include information about all surfaces, including vegetation and man-made structures.

Intensity Values: The peak power ratio of the laser return to the emitted laser, calculated as a function of surface reflectivity.

Nadir: A single point or locus of points on the surface of the earth directly below a sensor as it progresses along its flight line.

Overlap: The area shared between flight lines, typically measured in percent. 100% overlap is essential to ensure complete coverage and reduce laser shadows.

Pulse Rate (PR): The rate at which laser pulses are emitted from the sensor; typically measured in thousands of pulses per second (kHz).

Pulse Returns: For every laser pulse emitted, the number of wave forms (i.e., echoes) reflected back to the sensor. Portions of the wave form that return first are the highest element in multi-tiered surfaces such as vegetation. Portions of the wave form that return last are the lowest element in multi-tiered surfaces.

Real-Time Kinematic (RTK) Survey: A type of surveying conducted with a GPS base station deployed over a known monument with a radio connection to a GPS rover. Both the base station and rover receive differential GPS data and the baseline correction is solved between the two. This type of ground survey is accurate to 1.5 cm or less.

Post-Processed Kinematic (PPK) Survey: GPS surveying is conducted with a GPS rover collecting concurrently with a GPS base station set up over a known monument. Differential corrections and precisions for the GNSS baselines are computed and applied after the fact during processing. This type of ground survey is accurate to 1.5 cm or less.

Scan Angle: The angle from nadir to the edge of the scan, measured in degrees. Laser point accuracy typically decreases as scan angles increase.

Native LiDAR Density: The number of pulses emitted by the LiDAR system, commonly expressed as pulses per square meter.

Relative Accuracy Calibration Methodology:

Manual System Calibration: Calibration procedures for each mission require solving geometric relationships that relate measured swath-to-swath deviations to misalignments of system attitude parameters. Corrected scale, pitch, roll and heading offsets were calculated and applied to resolve misalignments. The raw divergence between lines was computed after the manual calibration was completed and reported for each survey area.

Automated Attitude Calibration: All data were tested and calibrated using TerraMatch automated sampling routines. Ground points were classified for each individual flight line and used for line-to-line testing. System misalignment offsets (pitch, roll and heading) and scale were solved for each individual mission and applied to respective mission datasets. The data from each mission were then blended when imported together to form the entire area of interest.

Automated Z Calibration: Ground points per line were used to calculate the vertical divergence between lines caused by vertical GPS drift. Automated Z calibration was the final step employed for relative accuracy calibration.

LiDAR accuracy error sources and solutions:

Type of Error	Source	Post Processing Solution
GPS (Static/Kinematic)	Long Base Lines	None
	Poor Satellite Constellation	None
	Poor Antenna Visibility	Reduce Visibility Mask
Relative Accuracy	Poor System Calibration	Recalibrate IMU and sensor offsets/settings
	Inaccurate System	None
Laser Noise	Poor Laser Timing	None
	Poor Laser Reception	None
	Poor Laser Power	None
	Irregular Laser Shape	None

Operational measures taken to improve relative accuracy:

Low Flight Altitude: Terrain following was employed to maintain a constant above ground level (AGL). Laser horizontal errors are a function of flight altitude above ground (about 1/3000th AGL flight altitude).

Focus Laser Power at narrow beam footprint: A laser return must be received by the system above a power threshold to accurately record a measurement. The strength of the laser return (i.e., intensity) is a function of laser emission power, laser footprint, flight altitude and the reflectivity of the target. While surface reflectivity cannot be controlled, laser power can be increased and low flight altitudes can be maintained.

Reduced Scan Angle: Edge-of-scan data can become inaccurate. The scan angle was reduced to a maximum of ±20^{o} from nadir, creating a narrow swath width and greatly reducing laser shadows from trees and buildings.

Quality GPS: Flights took place during optimal GPS conditions (e.g., 6 or more satellites and PDOP [Position Dilution of Precision] less than 3.0). Before each flight, the PDOP was determined for the survey day. During all flight times, a dual frequency DGPS base station recording at 1 second epochs was utilized and a maximum baseline length between the aircraft and the control points was less than 13 nm at all times.

Ground Survey: Ground survey point accuracy (<1.5 cm RMSE) occurs during optimal PDOP ranges and targets a minimal baseline distance of 4 miles between GPS rover and base. Robust statistics are, in part, a function of sample size (n) and distribution. Ground survey points are distributed to the extent possible throughout multiple flight lines and across the survey area.

50% Side-Lap (100% Overlap): Overlapping areas are optimized for relative accuracy testing. Laser shadowing is minimized to help increase target acquisition from multiple scan angles. Ideally, with a 50% side-lap, the nadir portion of one flight line coincides with the swath edge portion of overlapping flight lines. A minimum of 50% side-lap with terrain-followed acquisition prevents data gaps.

Opposing Flight Lines: All overlapping flight lines have opposing directions. Pitch, roll and heading errors are amplified by a factor of two relative to the adjacent flight line(s), making misalignments easier to detect and resolve.